

Authors' responses to reviewer's comments follow. A copy of the reviewer comment is given (with comment 'number') followed by a response (blue font).

Response to referee 1

1. General comments

The manuscript discusses radiocarbon estimated fossil fuel CO₂ emissions from local South Korean sources as well as from the Asian continent based on samples taken at the GAW station Anmyeondo in Korea. Additionally, they calculated the emission ratios of CO/CO₂ and SF₆/CO₂ and draw conclusions about improved oxidation efficiency in both the Asian continent as well as Korea. They also state based on a comparison between top-down and bottom-up (inventory) methods that there is a mismatch of estimated emissions to the point that inventory-based methods lead to up to 1.8 times lower emissions. The paper is well written, easy to follow and well-illustrated with graphs. I suggest publications of this manuscript after minor revision:

We thank you for your comments on the paper's value. We also appreciate your helpful comments to improve our manuscript. According to your specific comments, we revised our manuscript.

2. L:434 In South Korea and China, atmosphere-based RCO values are 1.2 times and (1.8±0.2) times greater than in the inventory, respectively. Please add also an uncertainty for the Korean value.

Thank you for the comment. We calculated each uncertainty for each sector. And we revised the sentence below.

Line 480: In South Korea and China, atmosphere-based R_{CO} values calculated by this study are (1.2±0.3) times (with KL), (1.6±0.4), (1.7±0.4), (2±0.1) and (1.7±0.2) times greater (with CB, CN, CE and OB) than in the inventory, respectively (Figure 4).

Also in the abstracts

Line 33: ...originating in China showed (1.6 ± 0.4) to (2 ± 0.1) times greater R_{CO} than...

In summary as well,

Line 516: For CO, our values are (1.2 ± 0.3) times and (1.6 ± 0.4) to (2 ± 0.1) times greater ...

3. L: 38 the CO₂ increase rate seems very high to me with a large uncertainty, 2.4 ± 0.5 ppm.

Thank you for the comment. Recently atmospheric CO₂ growth rate increased faster than the early measurement period, 1960s (0.8 ± 0.3 ppm/year). ± 0.5 is not uncertainty, rather the standard deviation of the annual increases. The value of S.D was a typo and should be ± 0.4 .

Line 41: atmosphere at (2.4 ± 0.4) $\mu\text{mol mol}^{-1} \text{a}^{-1}$ in a recent decade globally (where 0.4 is the standard deviation of annual growth rates; www.esrl.noaa.gov/gmd/ccgg/trends/, last access: 6 December 2019).

From 2010 to 2019, the CO₂ global annual increase

Year	2010	2011	2012	2013	2014	2015	2016	2017	2018	2019	Mean (\pm S.D.)
ppm/year	2.4	1.7	2.4	2.4	2.0	3.0	2.9	2.1	2.4	2.6	2.4 ± 0.4

These values are from www.esrl.noaa.gov/gmd/ccgg/trends/, as we cited in the manuscript.

4. L: 56 . . . , since those (not clear what you mean here, I guess CO₂)

Corrected.

Line 60: We revised it from ‘those emissions’ to ‘fossil fuel CO₂ emissions’

5. L:82-83 Why was the station location changed between the previous and the present study?

The TAP station does not belong to the KMA/NIMS and this paper focuses only on data from AMY. Therefore we think our data can give the information of this region with recent data since AMY is close to TAP (28 km away from AMY). We did not add that specific information in the manuscript.

6. L:126-127: what about permeation problems associated with glass flasks? To which pressure are the flasks filled? Under which conditions are the flask stored until measurement take place? How long does it take to be analysed?

The flasks have undergone extensive laboratory testing to ensure they maintain sample integrity for storage times up to one year. Comparison of flask-air samples with in situ measurements at South Pole have revealed storage offsets of up to 0.2 ppm after a year, but storage times at AMY are much less, and the difference in pressure between the flask and outside air (the main driver of preferential diffusion through the Teflon o-rings) is also less.

Flask-air sampling steps are as follows;

Using a semi-automated sampler, flasks are flushed at 5-6 L/min for 10 min then pressurized to 5 – 6 psig. After the pump turns off, falling pressure indicates a leak at the connectors. In that case, flasks are reconnected and the sample collected again. To prevent a slow leak through the pump, we close the stopcocks from the pump and to the exhaust first (esrl.noaa.gov/gmd/ccgg/psu/manuals/psu_manual_1.6.pdf). We store the collected samples in the laboratory and send them to NOAA about every two months.

Another reason we are sure there is no permeation problem is that we compare the flask-air CO₂ data to KMA continuous measurements. We confirmed the differences are small close to GAW's compatibility goal (± 0.1 ppm; Lee et al., 2019).

We added the sentence in the manuscript

Line 114: Two pairs of flask-air samples (4 flasks total, 2 L, borosilicate glass with Teflon O-ring sealed stopcocks) were collected about weekly from a 40 m tall tower at AMY, regardless of wind direction and speed from May 2014 to August 2016, generally between 1400 to 1600 local time (Table S1) using a semi-automated portable sampler. A pair of flasks was flushed for 10 min at 5-6 L min⁻¹ then pressurized to 5.5 psig in less than 1 min. A second pair is collected shortly after the first (within 20 min). The portable sampler was checked for leaks after pressurizing by observing the pressure gauge before closing the stopcocks. Batches of sampled flasks were shipped to Boulder, CO, USA every two months.

Line 136: When we compare NOAA's CO₂ measurements from flask-air with quasi-continuous measurements by KMA at AMY, the difference was -0.11 ± 2.32 $\mu\text{mol mol}^{-1}$ (mean ± 1 σ), close to GAW's compatibility goal for CO₂ (± 0.1 ppm for Northern Hemisphere measurements, Lee et al., 2019).

Reference: www.esrl.noaa.gov/gmd/ccgg/flask.html

7. L:164-166: It might be worthwhile to give a upper limit estimate for this influence. Maybe, also CO₂ flux values for the Yellow and Japanese Sea would be helpful for the reader to underpin your conclusion.

We agree with the reviewer It would be great to test whether the samples were affected by ocean fluxes, but this is well-beyond this study. So we added more references. There is a reference value of a flux that estimate for the East China Sea of -4.2 mmol/m²/day (Song et al., 2018). This value is very negligible. Turnbull et al. (2009) reported no significant bias from oceans in the Northern Hemisphere, even at coastal sites, while this bias is very important in the Southern Hemisphere. Also Turnbull et al. (2011a) mentioned that ocean exchange was negligible at TAP. Therefore we just added this reference in the manuscript and explained the bias from the ocean can be negligible.

Line 184: It was also demonstrated there is no significant bias from the oceans including

East China Sea (Song et al., 2018), even at coastal sites in Northern Hemisphere (Turnbull et al., 2009).

8. Eq. 4-6 I guess these equations are well-known and not necessary to be shown again. I would skip it and only reference on a paper describing this or to the software tool that you have used to calculate the regressions.

We deleted and added the reference. On the other hand, to make readers understand easily, we described the equations in the supplementary materials.

Line 201: we use reduced major axis (RMA) regression analysis (Sokal and Rohlf, 1981)

Line 205: The relevant equations are presented from Equ. S1 to Equ. S3.

Delete the equations from Line 207 to 217

9. L:309-310 This is an important issue to be discussed in more detail, since this relevant with the conclusions drawn from the data about Asian emissions.

It is very clear that even the C_{ff} from CB sector in this study increased compared to TAP far-field samples from 2004/2010. CB sector is the cleanest sector in this study with high wind speed (median value is 5 m/s and maximum of 10.2 m/s) and high PBL (median value is 600 m and maximized up to 1700 m). Therefore we assumed that any contamination could not affect the samples due to synoptic condition. For other sector which are originated from China, not only this study but also other studies showed the increased values compared to the Turnbull et al.(2011a).

But we did not totally ignore the possibility. As reviewer mentioned, it would be great to mention about those factors in more detail and to consider for further study.

Line 347: On the other hand, those values from this study showed large variability with small sample numbers due to different sampling strategy, environment, and synoptic

conditions such as boundary layer height at the sampling time from reference studies.

Further study will be necessary to understand those increased values.

10. L:314 what about correlation between SF₆ and CO?

When we implement RMA analysis for CO/SF₆, the correlation is very weak (R=0.18). And to consider only the outflow of Asian continent, R was 0.24. Only CE and OB whose CO and SF₆ had a good correlation with C_{ff} showed good correlation (R>0.6).

11. L: 337 what about a contamination from the local SF6 emissions on the ratio assigned to the Asian continent? Could you get an handle on it from SF6/CO ratios?

We considered this idea, when analyzing the R_{gas} values. But it was not possible due to several reasons. 1) as we explained, basically the correlation between SF₆ and CO was weak. 2) To select the data with SF₆/CO ratio, the ratios of sample-by-sample should be constant (or Gaussian). However the data characteristics did not show that.

Therefore to reduce local SF₆ effects, after cluster analysis we select the data again for wind speed > 3 m/s, as described in section 3.2. As seen in Table 1, the mean value and standard deviation of SF₆ in outflow from the Asia continent is smaller than for South Korea. This also means that SF₆ values was not be affected by local effects as shown by relatively constant values. We have high confidence that ratios from the Asian continent are less affected by local pollution.

12. Fig. 2 How sensitive are the results on the selection of the background values? To use NWR as background sounds rather strange as the two stations are very far apart and the authors mention explicitly Chinese station as well. Alternatives would be a Japanese location? or a European station. Or even lower bound values of the AMY station based on Hysplit selection.

When we selected the baseline station, there were only a few possible stations where ¹⁴C in CO₂ data were available. Asian stations would be a good option for this study but there is no available ¹⁴C data. And even if a data set existed, when the sampling/analysis methods are different, the

data uncertainty can be increased. Therefore we used NWR data, which are located at similar latitude to AMY with the same sampling/analysis method used as at AMY. And the analysis for ^{14}C was conducted by the same institute, INSTAAR, thus decreasing uncertainty that might occur if measurements from different laboratories were used (Miller et al., 2013)

According to Turnbull et al. (2011a), choice of background values did not significantly influence derived enhancements due to the large regional and local signal at TAP, 28 km from AMY. It was also described on Line 160. We hope the reviewer can understand that ^{14}C data are limited, and this is the one of reasons which makes this paper valuable.

Reference: Miller et al., (2013), Initial results of an intercomparison of AMS-Based atmospheric $^{14}\text{CO}_2$ measurements, Radiocarbon, Vol.55, Nr 2-3, 2013, 1475-1483.

13. Table 1 strange that r is low for PL trajectories. Has it to do with only a few values, since there is a much larger addition of fossil fuel CO_2 present.

When sampling well-mixed air masses, we can clearly see correlations among the gases. Under stagnant conditions, due to micro scale meteorology, the gases showed correlated weakly.

Authors' responses to reviewer's comments follow. A copy of the reviewer comment is given (with comment 'number') followed by a response (blue font).

Response to referee 2

1. General comments

This is a well-written paper with interesting data concerning atmospheric observations and validations of fossil CO₂, and CO and SF₆ emissions from Korea, and the Asian main land. Upon reading, I have made notes and comments that I present below. A more general remark (also given below) is that I invite/encourage the authors to more explicitly conclude what their observations show concerning the quality of the inventories, and if these inventories are thrus worthy or not. By drawing conclusions in that style, these data will be more accessible and valuable to policy makers, and might help to improve the inventories. I recommend publication after the authors have dealt with my comments below.

We thank you for your comments on this paper's value. We also appreciate your helpful comments to improve our manuscript. According to your specific comments, we revised our manuscript.

2. page 5, lines 108-109. at what flow rate are the flasks filled, or rather: is the flask air composition an average over some period of time, or merely a point in time?.

Samples are collected with a semi-automated sampler that first flushes the flasks at 5-6 L/min for 10 minutes then pressurizes them to 5.5 psig (5-6 LPM) in less than 1 min. Therefore, samples are integrated over 1-2 min.

We added the sentence on line 114.

Line 114: Two pairs of flask-air samples (4 flasks total, 2 L, borosilicate glass with Teflon O-ring sealed stopcocks) were collected about weekly from a 40 m tall tower at AMY, regardless of wind direction and speed from May 2014 to August 2016, generally between 1400 to 1600 local time (Table

S1) using a semi-automated portable sampler. A pair of flasks was flushed for 10 min at 5-6 L min⁻¹ then pressurized to 5.5 psig in less than 1 min. A second pair is collected shortly after the first (within 20 min). The portable sampler was checked for leaks after pressurizing by observing the pressure gauge before closing the stopcocks, Batches of sampled flasks were shipped to Boulder, CO, USA every two months

3. line 107 "Two pairs of flask-air samples (4 flasks total," In tabel S1 I see only one value per week. Is this an average? Flasks taken together for 14C mm?

We collect 4 samples but 2 among them were analyzed for ¹⁴C in CO₂. Among four flasks, the air from two flasks, after analysis for greenhouse gas mole fractions, was combined and analyzed for Δ(¹⁴CO₂)

Therefore we added the relevant sentence on Line131

Line144: Among four flasks, the air from two flasks, after analysis for greenhouse gas mole fractions, was combined and analyzed for Δ(¹⁴CO₂)

4. line 129 "suggested" ??

Line 144 we revised it to" tabulated"

5. line 245, 246 This largest positive C_{bio} is actually a single point. Which trajectory belongs to this point? The tic marks in the histogram of fig 2C do not correspond to those in the left part of fig 2C.

The largest positive value of C_{bio} is observed on August 2 2016 as shown in Figure 2. And it was observed in PL sector. To make it clear we revised the sentence line 279.

Line 287: The highest C_{bio} value was also observed in summer, PL sector.

Thank you for pointing out the y-axis ticks. We revised Figure 2 as below.

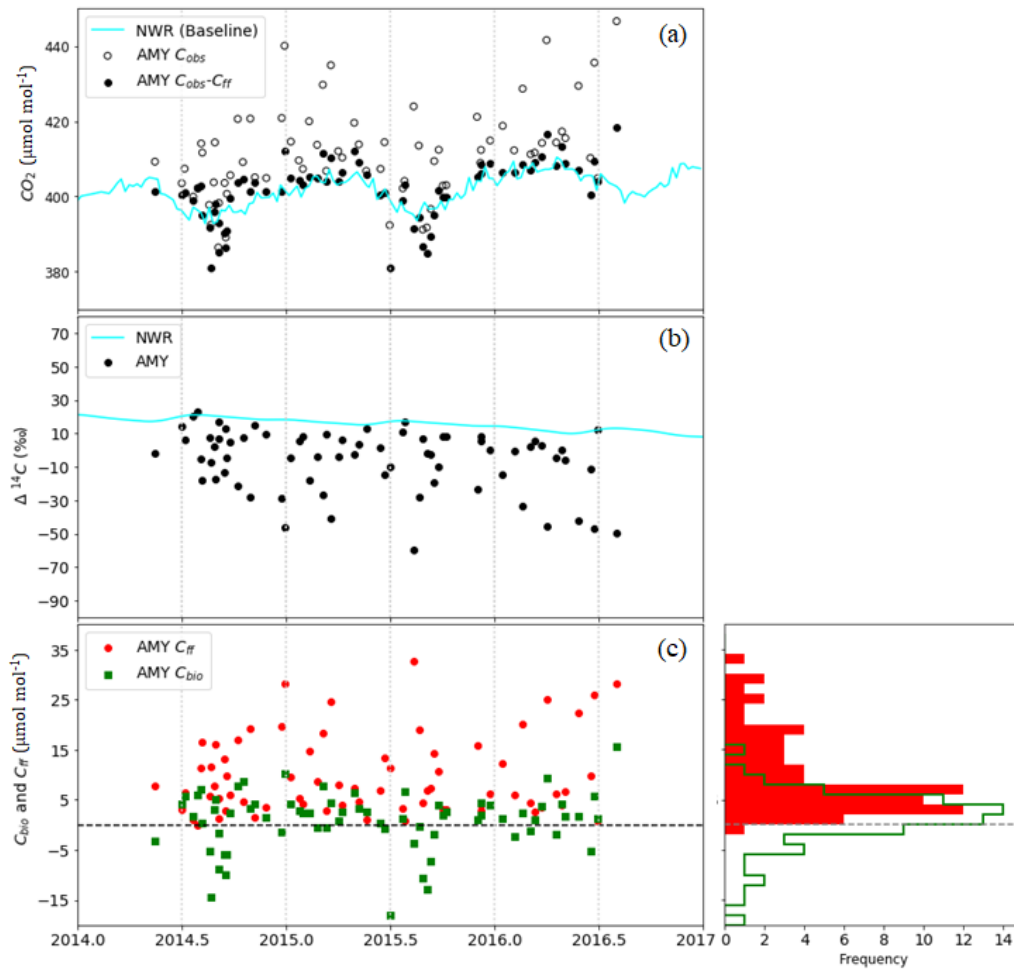


Figure 2. Time series of (a) observed CO_2 dry air mole fraction (open circles) and observed CO_2 (C_{obs}) minus C_{ff} calculated from $\Delta(^{14}\text{CO}_2)$ (closed circles). (b) $\Delta(^{14}\text{CO}_2)$ at AMY (black circles) and at NWR (Niwot Ridge, line), baseline data. (c) Time series of C_{ff} and C_{bio} calculated from $\Delta(^{14}\text{CO}_2)$ (left) and the frequency distribution at AMY (right).

6. Lines 252-254. I doubt the explanation offered. Even though your sampling time is early afternoon, I expect still the average mixing height to be the most important player in the mixing ratios of C_{ff} and C_{bio} , as it influences the flux-to-mixing ratios relation. There must be a seasonal effect in the mixing height no doubt. This must be taken into account in this discussion. The fact that C_{bio} covaries with C_{ff} also points to the importance of the (average) mixing height.

We agreed with reviewer's comments. When we analyzed the PBL height for each sample by meteorological model, winter was highest (with a range from 150 m to 1100 m) and summer/spring are lower than other seasons (with a range from 100 m to 800 m). This result is consistent with the explanation of wind speed in the manuscript. Therefore we added this sentence.

Line 282: When we analyzed seasonal boundary layer height for each sample by UM-GDAPS, it also showed similar result that it was highest in winter (with a range from 150 m to 1100 m) and lowest in summer (with a range from 100 m to 500 m). This suggests that these high summer C_{ff} values may reflect emission from local activities, which were described in section 2.1, more than in other seasons.

7. Line 270-271 I would say in general nobody expects the CO_2 enhancements above background to be entirely due to C_{ff} .

Thank you for the comment. The point is that regardless of the source and seasons, we find that C_{bio} contributes to atmospheric CO_2 enhancements at AMY. And if we just use CO_2 enhancements to demonstrate the bottom-up inventory, it can be biased. Therefore we emphasized this in section 4. "Finally, we stress that because C_{bio} contributes substantially to $\Delta x(CO_2)$, even in winter, $14C$ -based C_{ff} (and not $\Delta x(CO_2)$) is required for accurate calculation of both R_{CO} and R_{SF6} ."

To avoid the confusion, we revised the explanation in the section directly on line 302

Line 302: ... so when only CO_2 enhancements above background are compared to bottom-up inventories, it can make a bias due to C_{bio} contributions.

8. Line 280-282 "During the experimental period, the averages from Asian continent (sectors CE and CN) were higher than KL without the baseline level." Without the baseline level?? What do you mean?

"Without baseline" means that Continental Baseline (CB) and Ocean Baseline (OB) sector.

We added the explanation on line 316,

Line 316: ...without baseline sector (CB and OB)

9. Does OB fit in this set? You call it ocean background, but at the same time you mention it crosses over Shanghai (213-214). In line 234-235 you indicate it again as being background, and then here (282) you take it along with the "real" continental trajectories. This needs to be clarified.

We agree. The cluster definitely belongs to Ocean Background, but some of the air masses (4 of 10) have paths over southern China, such as Shanghai. We confirmed that the altitudes that air masses came through were high enough when over southern China that they were unlikely affected by surface sources and sinks. But we cannot ignore the possibility that these trajectories could have affected our results. We revised the sentence below:

Line 239: .Among them, a few of the trajectories passed over the eastern part of China (e.g., over Shanghai) with high altitude (~1000 m).

10. 298-299 "we also see CN originated from northeast China and it was around $(10.6 \pm 6.9) \mu\text{mol mol}^{-1}$." I don't get the meaning or consequence of this sentence part.

A previous study mentioned that northeast China affected SDZ-NE sector samples and they showed $(3 \pm 7) \mu\text{mol mol}^{-1}$ in 2009 to 2010 and increased to $(7.6 \pm 6.8) \mu\text{mol mol}^{-1}$ in 2015.

In this study, samples originated from northeast China (NE) showed increased C_{ff} levels around $(10.6 \pm 6.9) \mu\text{mol}$ compared to 2009 to 2010.

We revised the sentence clear

Line 333: we also see CN that originated from northeast china (NE) and its mean value of C_{ff} had increased around $(10.6 \pm 6.9) \mu\text{mol mol}^{-1}$ compared to those values in 2009 to 2010.

11. Lines 300-302 Once more, I think average mixing height is the key player here. Are the weather patterns, and thus mixing heights different in the years 2009-2010 from 2014-2106? Did Turnbull et al also sample between 14 and 16 hours?

Turnbull et al. (2011a) sampled flasks during mid-afternoon, so that we assume the sampling time might be similar. One difference is they collected air when there was an onshore wind while in this study, samples were collected regardless of wind direction and speed.

We could not research the mixing height in 2009 to 2010, but it is very clear that C_{ff} from CB sector in this study increased compared to TAP far-field samples from 2004/2010. CB sector is the cleanest sector in this study with high wind speed (median value is 5 m/s, with a maximum of 10.2 m/s) and high PBL (median value is 600 m, with a maximum of 1700 m). There is no possibility for local-scale pollution to affect the samples due to the synoptic conditions.

Other sectors that originated from China, not only in this study, but also other studies, showed increased values compared to Turnbull et al. (2011a).

On the other hand, we also considered the possibility of unexpected conditions that could affect this analysis. ***Line 345: It is also likely that the proximity of local emission sources to AMY is causing higher observed C_{ff} under some synoptic conditions.***

As the reviewer mentioned, it would be great to mention those factors in more detail and the importance for further study, so we removed the sentence above and added:

Line 347: On the other hand, those values from this study showed large variability with small sample numbers due to different sampling strategy, environment, and synoptic

conditions such as boundary layer height at the sampling time from reference studies.

Further study will be necessary to understand those increased values.

12. 304 increase of 16.7% line306 "broadly consistent" I disagree for the China case, as you find way larger increases between 2010 and 2016. So you might hypothesize that your measurements indicate much higher increases in fossil fuel use? Of course what you state in 311-312 is very true...

We also pointed out the Asia main land differently from Korea Local air.

Line 341: This is broadly consistent with the flat trend in observed C_{ff} in KL air masses, and in the upward trend in C_{ff} observed in air-masses flowing out from Asia.

We also explained the possibilities to affect this result on line 347. Therefore we did not revise the sentence.

13. Line 321 are these differences significant? I would say $(KL, PL) > (CN, CE) > (CB, OB)$

Line358: Corrected

14. Line 331 To my opinion SF_6 is not a good tracer/surrogate for fossil fuel CO_2 , as it is not produced in the same process. So SF_6 actually traces specific industrial activities, and electricity use. Both are coupled to fossil fuel CO_2 , but not in a 1:1 (spatial, temporal) relation. CO , on the other hand is really co-produced with fossil fuel CO_2 (and with biofuel CO_2), albeit at a varying rate.

Though the reviewer's comment is true, it is also true that C_{ff} and ΔSF_6 correlate quite strongly in CE, OB and KL sectors. This means even if they don't have a same source, they are emitted from similar regions. Therefore, we suggest that ΔSF_6 can be a proxy of fossil fuel CO_2 in those regions. But as you mentioned ΔSF_6 cannot always a good tracer of fossil fuel CO_2 , so we revised the sentence as below.

We revised line 362:

Line 372: Thus SF₆ can be a good tracer of fossil fuel CO₂ for those regions.

15. Line 332 "Even though" I don't see the contrast between the strong correlation and the differences

The correlation was strong in both South Korea and for the Asian continent, but the R value was totally different for both regions.

We revised line 373:

Line 373: The correlation between $\Delta x(\text{SF}_6)$ and Cff was strong in CE, OB and KL, however, R_{SF6} is different between South Korea and outflow from the Asian continent (Figure S2).

16. Caption figure S3: "From 2005,.. " -> "From 2005 onwards, .."

Corrected.

17. lines 347-349 Still, in spite of the still large uncertainty, I invite you to make a stronger statement here, namely that the SF₆ inventory in EDGAR and in KNIR are too low given your measurements.

We revised the sentence here

Line 388: Even though KL R_{SF6} showed greater uncertainty than CE and OB, it is still greater than bottom-up inventories, such as KNIR and EDGAR. Therefore it would be useful to get more data to try and derive a more robust estimate to evaluate SF₆ emission inventories for Korea.

18. Line 351 also here, watch the significance. I would conclude from table 1 that CB=KL. And indeed

(see my point higher up), OB is mostly regional background air.

Corrected (Line 395).

For OB sector, we revised the explanation according to reviewer's comment No.9 above.

19. 354 "CO...it is more closely related to fossil fuel CO₂ emissions" yes, but also to biomaterial combustion (compare the C_{ff} to the CO excess)

We agree. The revised sentence below

Line 397: Since CO is produced during incomplete combustion of fossil fuels and biomass, it is more closely related to fossil fuel CO₂ emissions than the other trace gases.

20. 357-358 I think you can safely erase the word "likely" here. 358 add "and the use of catalysers" ?

Corrected

Line 402 ... due to differences in combustion efficiencies and the use of catalytic converters

21. 358-360 Indeed, biomaterial combustion must play a role, regarding the low C_{ff} especially for CB.

We agree and added the following sentence.

Line 405: For example, for CB the CO level is similar to KL while R_{CO} is higher than KL with low C_{ff}.

22. 366 Figure S2 -> Figure S1

Corrected (Line 413).

23. 369 Paragraph 3.4 I suppose you did a similar thing for the SF6 inventories. That means the either the start of this paragraph should be moved up into 3.3, or the SF6 inventory discussions should be taken form 3.3 and moved to this paragraph.

Corrected. We separated two sections according to the species.

3.3 Correlation of Cff with SF6 and its emission ratios

3.4 Correlation of Cff with CO and its emission ratios

24. 377 "The uncertainty of EDGAR4.3.2 emissions" -> "The uncertainty of EDGAR4.3.2 fossil fuel CO2 emissions"

Corrected (Line 422)

25. 397-399 if a difference is not significant, it is doubtful to discuss its possible causes.

We removed the sentence from Line 443 to Line 444.

26. 403 "KNIR seems to have uncounted CO emissions," -> "KNIR suffers from a high number of missing CO emission sources," in other words: make this statement stronger, as the difference is huge: _2500 vs _700 Gg in 2012 ! And your data corroborate the Edgar emission ratios...

Corrected

Line 448: KNIR suffers from a large number of missing CO emission sources compared to the EDGAR, as indicated by their reported emissions, 638.3 and 2580.8 Gg in 2012, respectively

27. 433-439 S. Korea: your RCO results are 1.2 times the Edgar results. That is hard to see in figure 4.

Your value (from table 1) is 8 ± 2 , so a $\pm 25\%$ uncertainty, which makes this factor 1.2 not significant. The Chinese inventories, on the other hand, ARE significantly too low, even though the declining trend has been confirmed by atmospheric measurements. My guess would be that the lack of biofuels/biomaterial burning which is not present in the EDGAR CO inventory, explains the large difference in China, and is not so important in S. Korea.

We agree reviewer's comment for two reasons. First, EDGAR does not reflect secondary CO production and, second, CO derived from biomass burning and biofuels was not included by EDGAR. Since we described it already, we did not revise the sentence. This is described in the manuscript as:

Line 485: Also, CO derived from biomass burning and biofuels was not included in this inventory. Therefore, this indicates that top-down observations are necessary to evaluate and improve bottom-up emission products.

28. 441 (and also earlier and further) you express mean values \pm standard deviations, whereas the way you write it suggests that this is the error in the mean value, which is in fact \sqrt{n} lower. So in fact the mean value here is $(-6.2 \pm 2.2) \text{‰}$ (I took $N=70$), with a spread of 19‰. In your case, most of the time the spread= the standard deviation is the important feature, but if you compare in lines 446-447 to previous measurements at TAP it is important to know how many measurements those were, and thus what the mean and error in the mean are. Your statement: the average is twice as high strongly suggests that this difference is significant, but the reader can only judge that if you present the error in the mean in both cases. I advise to make this difference between standard deviation and error in the mean clear at the various points where it matters in the paper.

Thank you for your comment. It is very true that standard deviation (SD) and standard error of the mean (SEM) are totally different. The reference values from Turnbull et al. (2011a) and Niu et al. (2016) were also SD rather than SEM, which we verified in their publications.

As the reviewer already commented, SD is the dispersion of data in normal distributions. In other words, SD indicates how accurately the mean represents sample data. For SEM, it is the SD of the

theoretical distribution of the sample mean (the sampling distribution).

In this regards, it would be good to use SEM though, however, since the data set we used here is not continuous, only weekly resolution, the number of data is quite small for SEM. When we use SEM, the data characteristics can be underestimated because the error can be decreased, certainly. The number of data is very limited that dispersion of data can be important information for reader.

Therefore we just added the number of the data for the calculation (since whether we use SD or SEM, this is very important information) and retain SD.

Please see the revised manuscript. When previous studies did not include the number of data, we could not include it.

29. Lines 449-452 Yes, C_{ff} really increased for the air masses from the Asian mainland. Do you conclude that this indicates stronger growth of fossil fuel use than the statistics say? If you think your data clearly point at that, mention that here.

The atmospheric C_{ff} was increased compared to the previous studies but we cannot explain that our results are much greater than the reported inventory values. When we analyze inverse modeling, we can point it clearly. Therefore we revised sentence in section 4, 2).

Line 502: After separately identifying samples originating from the Asian continent and the Korean peninsula, we determined that the mean C_{ff} increased relative to the earlier observations due to increased fossil fuel emissions from the Asian continent as showing the consistent growth with reported emission increased 16.7% in China while 1.8% in South Korea from 2010 to 2016.

30. lines 453-463 Based on your data I would (also) conclude the following: (1) ^{14}C analysis is a reliable way of determining C_{ff} in the mixing ratio of air masses (2) Then, the ratio of the emission of rare trace gases and C_{ff} can be determined as well (3) As the inventories for various other trace gases/greenhouse gases are generally much less reliable than that of C_{ff} , these inventories can

be validated/verified using atmospheric measurements like ours. (4) In our case we conclude that the inventories for SF₆ ... and for CO ... In this way your results will probably be more valuable to policy makers. would also formulate (part of) this reasoning in the abstract.

We re-write the summary and conclusion according to reviewer's comment.

Please see the revised the version of section 4 and abstract as well.

31. Two more references suggested: Page 2 I would suggest in addition the reference : van der Laan, S. et al. Observation based estimates of fossil fuel-derived CO₂ emissions in the Netherlands using Delta 14C, CO and 222Radon, Tellus B, 62(5, SI), 389–402, doi:10.1111/j.1600-0889.2010.00493.x, 2010.

We added the reference.

32. page 3 line 64 "...correlate well..." I think the earliest 14C-based reference to this is Zondervan, A. and Meijer, H. A. J.: Isotopic characterisation of CO₂ sources during regional pollution events using isotopic and radiocarbon analysis, TELLUS SERIES BCHEMICAL AND PHYSICAL METEOROLOGY, 48(4), 601–612, doi:10.1034/j.1600-0889.1996.00013.x, 1996.

We added the reference.

~~¹⁴C—observations—~~Observations of atmospheric ¹⁴CO₂ at Anmyeondo GAW station, Korea: Implications for fossil fuel CO₂ and emission ratios

Haeyoung Lee^{1,2}, Edward J. Dlugokencky³, Jocelyn C Turnbull^{4,5}, Sepyo Lee¹, Scott J. Lehman⁶, John B Miller³, Gabrielle Petron^{3,5}, Jeongsik Lim^{7,8}, and Gang-Woong Lee², Sang-Sam Lee¹ and Young-San Park¹

Correspondence to Haeyoung Lee (leehy80@korea.kr)

¹National Institute of Meteorological Sciences, Jeju, 63568, Republic of Korea

²Atmospheric Chemistry Laboratory, Hankuk University of Foreign Studies, Gyeonggi-do, 17035, Republic of Korea

³NOAA, ~~Earth System Research Laboratory~~, Global Monitoring ~~Division~~Laboratory, Boulder, Colorado, USA

⁴National Isotope Center, GNS Science, Lower Hutt, New Zealand

⁵CIRES, University of Colorado, Boulder, Colorado, USA

⁶INSTAAR, University of Colorado, Boulder, Colorado, USA

⁷Korea Research Institute of Standard and Science, Daejeon, 34113, Republic of Korea

⁸University of Science and Technology, Daejeon, 34113, Republic of Korea

Abstract. To understand Korea's carbon dioxide (CO₂) emissions and sinks as well as those of the surrounding region, we used 70 flask-air samples collected during May 2014 to August 2016 at Anmyeondo (AMY, 36.53° N, 126.32° E; 46 m a.s.l.) World Meteorological Organization (WMO) Global Atmosphere Watch (GAW) station, located on the west coast of South Korea, for analysis of observed ¹⁴C in atmospheric CO₂ as a tracer of fossil fuel CO₂ contribution (C_{ff}). Observed ¹⁴C/C ratios in CO₂ (reported as Δ values) at AMY varied from -59.5 to 23.1 ‰ with the measurement uncertainty of ±1.8 ‰. The derived mean value C_{ff} of (9.7 ± 7.8) μmol mol⁻¹ (1σ) is greater than that found in earlier observations from Tae-Ahn Peninsula (TAP, 36.73° N, 126.13° E, 20 m a.s.l., ~~24–28~~ km away from AMY) of (4.4 ± 5.7) μmol mol⁻¹ from 2004 to 2010. The enhancement above background of sulfur hexafluoride (Δx(SF₆)) and carbon monoxide

$(\Delta x(\text{CO}))$ correlate strongly with C_{ff} ($r > 0.7$) and appear to be good proxies for fossil fuel CO_2 at regional and continental scales. Samples originating from the Asian continent had greater $\Delta x(\text{CO}):C_{\text{ff}}$ (R_{CO}) values, (29 ± 8) to (36 ± 2) $\text{nmol } \mu\text{mol}^{-1}$, than in Korean local air $((8 \pm 2) \text{ nmol } \mu\text{mol}^{-1})$. Air masses originating in China showed ~~(1.8 ± 0.2)~~ (1.6 ± 0.4) to (2 ± 0.1) -times greater R_{CO} than a bottom-up inventory suggesting that China's CO emissions are underestimated in the inventory while observed R_{SF_6} values are 2-3 times greater than inventories for both China and Korea. However, both R_{CO} derived from inventories and observations have decreased relative to previous studies, indicating that combustion efficiency is increasing in both China and South Korea.

1 Introduction

Carbon Dioxide (CO_2) is the principle cause of climate change in the industrial era, and is increasing in the atmosphere at $(2.4 \pm 0.54) \mu\text{mol mol}^{-1} \text{ a}^{-1}$ in a recent decade globally (where 0.4 is the standard deviation of annual growth rates; www.esrl.noaa.gov/gmd/ccgg/trends/, last access: 6 December 2019). This increase is by release of CO_2 from fossil fuel combustion in fact predominantly an anthropogenic disturbance that has been demonstrated through ^{14}C analysis of tree rings from the last two centuries (Stuiver and Quay, 1981; Suess, 1955; Tans et al., 1979); caused by accelerated release of CO_2 from fossil fuel burning. Atmospheric measurement program for the ratio $^{14}\text{C}/\text{C}$ in CO_2 was initiated in the 1950s and 1960s (Rafter and Fergusson, 1957; Nydal, 1996). Observed $^{14}\text{C}/\text{C}$ ratios are reported in Delta notation ($\Delta(^{14}\text{CO}_2)$) as fractionation-corrected permil (or ‰) deviations from the absolute radiocarbon standard

(Stuiver and Polach, 1977). Many studies show that the variation of $\Delta(^{14}\text{CO}_2)$ is an unbiased and now widely used tracer for CO_2 emitted from fossil-fuel combustion (Levin et al., 2003; Turnbull et al., 2006; Graven et al., 2009; [Van der Laan et al., 2010](#); Miller et al., 2012). Therefore measurements of $\Delta(^{14}\text{CO}_2)$ are important to test the effectiveness of emission reduction strategies to mitigate the rapid atmospheric CO_2 increase, since they can partition observed CO_2 enhancements, $\Delta x(\text{CO}_2)$, into fossil fuel CO_2 (C_{ff}) and biological CO_2 (C_{bio}) components with high confidence (Turnbull et al., 2006).

When trace gases are co-emitted with C_{ff} , correlations of their enhancements with C_{ff} improve understanding of the emission sources of both C_{ff} and the co-emitted tracers. For example, CO and CH_4 emission inventories are typically more uncertain than the fossil fuel CO_2 emission inventory, since [fossil fuel \$\text{CO}_2\$](#) emissions related to complete combustion are generally well estimated while emissions related to incomplete combustion and agricultural activities are poorly constrained (Kurokawa et al., 2013). Temporal changes in the observed emission ratio of a trace gas to C_{ff} can be used to examine emission trends in the trace gas (Tohijima et al., 2014). Therefore the observed emission ratios of trace gases to C_{ff} can be used to evaluate bottom-up inventories of various trace gases (e.g., Miller et al., 2012). Here, we used two trace gases, carbon monoxide (CO) and sulfur hexafluoride (SF_6) for this analysis. CO is produced along with CO_2 during incomplete combustion of fossil fuels and biomass. CO enhancements above background ($\Delta x(\text{CO}_2)$) correlate well with C_{ff} and have been used as a fossil fuel tracer ([Zondervan and Meijer, 1996](#); Gamnitzer et al., 2006; Turnbull et al., 2011a; Turnbull et al., 2011b; Tohijima et al., 2014). SF_6 is an entirely anthropogenic gas and is widely used as an arc quencher in high-voltage electrical equipment (Geller et al., 1997). At regional to continental scales, persistent small leaks to the atmosphere of SF_6 are typically co-located with fossil fuel

CO₂ sources and allow SF₆ to be used as an indirect C_{ff} tracer, if the leaks are co-located with C_{ff} emissions at the location and scale of interest (Turnbull et al., 2006; Rivier et al., 2006).

South Korea is a rapidly developing country with fast economic growth, and it is located next to China, which is the world's largest emitter of anthropogenic CO₂, ~~according to the Emissions Database for Global Atmospheric Research EDGAR~~ (Boden et al., 2017; Janssens-Maenhout et al., 2017). The first $\Delta(^{14}\text{CO}_2)$ measurements in South Korea were reported by Turnbull et al. (2011a) based on air samples collected during October 2004 to March 2010 at Tae-Ahn Peninsula (TAP, 36.73° N, 126.13° E, 20 m a.s.l.). This study showed that observed CO₂ at this site was often influenced by Chinese emissions and the observed ratio of $\Delta x(\text{CO}):C_{\text{ff}}$ (R_{CO}) was greater than expected from bottom-up inventories. However South Korean $\Delta(^{14}\text{CO}_2)$ data are still limited and the ratio of the other trace gases to C_{ff} barely discussed.

Here we use whole-air samples collected in glass flasks during May 2014 to August 2016 at Anmyeondo (AMY, 36.53° N, 126.32° E; 46 m a.s.l.) World Meteorological Organization (WMO) Global Atmosphere Watch (GAW) station, located on the west coast of South Korea and about 28 km SSE of TAP, where the first study was conducted. We decompose observed CO₂ enhancements into their fossil fuel and biological components at AMY to understand sources and sinks of CO₂. We also implemented cluster analysis using the NOAA Hybrid Single Particle Lagrangian Integrated Trajectory Model (HYSPLIT) to calculate back-trajectories for sample times and dates. Based on clusters of trajectories from specific regions, trace gas enhancement: C_{ff} ratios and correlation coefficients were analyzed, especially focused on SF₆ and CO, to determine the potential of alternative proxies to $\Delta(^{14}\text{CO}_2)$. Finally we compared our $\Delta x(\text{CO}):C_{\text{ff}}$ ratio with ratios determined from bottom-up inventories (EDGARv4.3.2 and Korea's National

Inventory Report in 2018) to evaluate reported CO emissions and how they've changed since 2010.

2. Materials and Methods

2.1 Sampling site and methods

The AMY GAW station is managed by the National Institute of Meteorological Sciences (NIMS) in the Korea Meteorological Administration (KMA). It has the longest record of continuous CO₂ measurement in South Korea, beginning in 1999. It is located on the west coast of Korea about 130 km southwest of the megacity of Seoul, whose population was 9.8 million in 2017. Semiconductor and other industries exist within a 100 km radius of the station. Also, the largest thermal power plants fired by coal and heavy oil in South Korea are within 35 km to the northeast and southeast of the station. The closest town, around 30 km to the east of AMY, is well known for its livestock industries. Local economic activities are related to agriculture, e.g., production of rice paddies, sweet potatoes, and onions, and the area is also known for its leisure opportunities that increase traffic and tourists in summer, indicating the complexity of greenhouse gas sources around AMY. On the other hand, air masses often arrive at AMY from the west and south, which is open to the Yellow Sea. Therefore AMY observes enhanced CO₂ compared to many other East Asian stations due not only to numerous local sources but also long-range transport of air-masses from the Asian continent (Lee et al., 2019).

Two pairs of flask-air samples (4 flasks total, 2 L, borosilicate glass with Teflon O-ring sealed stopcocks) were collected about weekly from a 40 m tall tower at AMY, regardless of wind

direction and speed from May 2014 to August 2016, generally between 1400 to 1600 local time (Table S1) using a semi-automated portable sampler. A pair of flasks was flushed for 10 min at 5-6 L min⁻¹ then pressurized to 5.5 psig in less than 1 min. A second pair is collected shortly after the first (within 20 min). The portable sampler was checked for leaks after pressurizing by observing the pressure gauge before closing the stopcocks. Batches of sampled flasks were shipped to Boulder, CO, USA every two months.

A total of 70 sets were collected and analyzed at the National Oceanic and Atmospheric Administration/Earth System Research Laboratory/Global Monitoring Division (NOAA/ESRL/GMD) for CO₂, CO, and SF₆ and for $\Delta(^{14}\text{CO}_2)$ by University of Colorado Boulder, Institute of Arctic and Alpine Research (INSTAAR). NOAA/ESRL/GMD analyzed CO₂ using a non-dispersive infrared analyzer, SF₆ using gas chromatography (GC) with electron capture detection, and CO by vacuum UV, resonance fluorescence. All analyzers were calibrated with the appropriate WMO mole fraction scales (WMO-X2007 scale for CO₂, WMO-X2014A scale for CO, and WMO-X2014 for SF₆; <https://www.esrl.noaa.gov/gmd/ccl/>, last access: 4 December 2019). The measurement and analysis methods for those gases are described in detail (http://www.esrl.noaa.gov/gmd/ccgg/behind_the_scenes/measurementlab.html, last access: 4 December 2019). Measurement uncertainties for CO₂ and SF₆ are reported as 68% confidential intervals. For CO₂, it is 0.07 $\mu\text{mol mol}^{-1}$ for all measurements used here. For SF₆, it is 0.04 ~~up to~~ ~~12~~ pmol mol^{-1} , ~~and undefined above that~~. For CO, measurement uncertainty has not yet been formally evaluated, but is estimated at 1 nmol mol^{-1} (68% confidence interval). All CO₂, SF₆ and CO data at AMY can be downloaded through ftp://aftp.cmdl.noaa.gov/data/trace_gases/. When we compare NOAA's CO₂ measurements from flask-air with quasi-continuous measurements by

KMA at AMY, the difference was $-0.11 \pm 2.32 \text{ } \mu\text{mol mol}^{-1}$ (mean $\pm 1 \text{ } \sigma$), close to GAW's compatibility goal for CO_2 ($\pm 0.1 \text{ ppm}$ for Northern Hemisphere measurements, Lee et al., 2019).

The analysis methods for $\Delta(^{14}\text{CO}_2)$ are described by Lehman et al. (2013). Measurement repeatability of $\Delta(^{14}\text{CO}_2)$ in aliquots of whole air extracted from surveillance cylinders is 1.8% ($1 \text{ } \sigma$), roughly equating to $1 \text{ } \mu\text{mol mol}^{-1}$ C_{ff} detection capability from the measurement uncertainty alone. The $\Delta(^{14}\text{CO}_2)$ data at AMY was ~~suggested~~-tabulated in Table S1. Among four flasks, the air from two flasks, after analysis for greenhouse gas mole fractions, was combined and analyzed for $\Delta(^{14}\text{CO}_2)$.

2.2 Data analysis method using $\Delta(^{14}\text{CO}_2)$ data

2.2.1 Calculation of C_{ff} and C_{bio}

As Turnbull et al. (2009) suggested the observed CO_2 (C_{obs}) at AMY can be defined as:

$$C_{\text{obs}} = C_{\text{bg}} + C_{\text{ff}} + C_{\text{other}} \quad (1)$$

where C_{bg} , C_{ff} and C_{other} are the background, recently added fossil fuel CO_2 and the CO_2 derived from the other sources.

According to Tans et al. (1993), the product of CO_2 abundance and its isotopic ratio is conserved; the isotopic mass balance can be described as below:

$$\Delta_{\text{obs}}C_{\text{obs}} = \Delta_{\text{bg}}C_{\text{bg}} + \Delta_{\text{ff}}C_{\text{ff}} + \Delta_{\text{other}}C_{\text{other}} \quad (2)$$

where Δ is the $\Delta^{14}\text{C}$ of each CO_2 component of Equ. (1).

Therefore we can calculate fossil fuel CO_2 by combining equations (1) and (2) as:

$$C_{\text{ff}} = \frac{C_{\text{bg}}(\Delta_{\text{obs}} - \Delta_{\text{bg}})}{\Delta_{\text{ff}} - \Delta_{\text{bg}}} - \frac{C_{\text{other}}(\Delta_{\text{other}} - \Delta_{\text{bg}})}{\Delta_{\text{ff}} - \Delta_{\text{bg}}} \quad (3)$$

Fossil fuel derived CO_2 contains no ^{14}C because the half-life of ^{14}C is (5700 ± 30) years (Godwin, 1962) while these fuels are hundreds of millions of years old. As we mentioned in the section 1, $\Delta(^{14}\text{CO}_2)$ is reported as a per mil (‰) deviation from the absolute radiocarbon reference standard corrected for fractionation and decay with a simplified form; $\Delta(^{14}\text{C}) \approx [(^{14}\text{C}/\text{C})_{\text{sample}} / (^{14}\text{C}/\text{C})_{\text{standard}} - 1]1000\text{‰}$. Therefore Δ_{ff} is set at -1000‰ (Stuiver and Pollach, 1977). Background values (Δ_{bg}) in equations (1) to (3) are determined from measurements from background air collected at Niwot Ridge, Colorado, a high altitude site at a similar latitude as AMY (NWR, 40.05° N , 105.58° W , 3,526 m a.s.l.). Turnbull et al. (2011a) showed that the choice of background values did not significantly influence derived enhancements due to the large regional and local signal at TAP, 28 km from AMY. NWR $\Delta(^{14}\text{CO}_2)$ and other trace gas background values are selected using a flagging system to exclude polluted samples (Turnbull et al., 2007), and then fitted with a smooth curve following Thoning et al. (1989).

The second term of equation (3) is typically a small correction for the effect of other sources of CO_2 that have a $\Delta^{14}\text{C}$ differing by a small amount that of the atmospheric background, such as

CO₂ from the 1) nuclear power industry, 2) oceans, 3) photosynthesis and 4) heterotrophic respiration.

1) The nuclear power industry produces ¹⁴C that can influence the C_{ff} calculation. South Korea has nuclear power plants along the east coast that may influence AMY air samples when air masses originated from the eastern part of Korea (Figure 1). It is also possible that Chinese nuclear plants could influence some samples. Here we did not make any correction for this since most nuclear installations in this region are pressurized water reactors, which produce mainly ¹⁴C in CH₄ rather than CO₂ (Graven and Gruber, 2011). 2) For the ocean, although there may also be a small contribution from oceanic carbon exchange across the Yellow Sea, we consider this effect small enough to ignore (Turnbull et al., 2011a). It was also demonstrated there is no significant bias from the oceans including East China Sea (Song et al., 2018), even at coastal sites in the Northern Hemisphere (Turnbull et al., 2009). Larger scale ocean exchange and also stratospheric exchange affect both background and observed samples equally, so they can be ignored in the calculations. 3) For the photosynthetic terms, ¹⁴C in CO₂ accounts for natural fractionation during uptake, so we also set this observed value the same as the background value. 4) Therefore we only consider heterotrophic respiration. For land regions, where most fossil fuel emissions occur, heterotrophic respiration could be a main contributor to the second term of equation (3) due to ~~large~~ ¹⁴C disequilibrium potentially. When this value is ignored, C_{ff} would be consistently underestimated (Palstra et al., 2008; Riley et al., 2008; Hsueh et al., 2007; Turnbull et al., 2006). For this, corrections were estimated as (-0.2±0.1) μmol mol⁻¹ during winter and (-0.5±0.2) μmol mol⁻¹ during summer (Turnbull et al., 2009; Turnbull et al., 2006).

CO₂ enhancements relative to baseline CO₂ are defined as $\Delta x(\text{CO}_2)$, with the excess signal of C_{obs} minus C_{bg} in Equ.(1). Partitioning of $\Delta x(\text{CO}_2)$ into C_{ff} and C_{bio} is calculated simply from the residual of the difference between observed $\Delta x(\text{CO}_2)$ and C_{ff} .

2.2.2 The ratio of trace gas enhancement to C_{ff} and its correlation

To obtain the correlation coefficient (r) between C_{ff} and other trace gas enhancements ($\Delta x(x) = x_{\text{obs}} - x_{\text{bg}}$) and the ratio of any trace gas to C_{ff} (R_{gas}), we use reduced major axis (RMA) regression analysis (Sokal and Rohlf, 1981). The distributions of R_{gas} are normally broad and non-Gaussian and RMA analysis is a relatively robust method of calculating the slope of two variables that show some causative relationship. Here, x_{bg} was derived from NWR with the same method described in section 2.2.1. The relevant equations are presented from Equ. S1 to Equ. S3. Results for each species are given in Table 1.

~~Here, x_{bg} was derived from NWR with the same method described in section 2.2.1.~~

~~Therefore, the slope of the linear regression of the RMA fit can be expressed as~~

$$R_{\text{gas}} = \frac{\sqrt{\frac{\sum \Delta x(x)^2 - (\sum \Delta x(x))^2/n}{\sum C_{\text{ff}}^2 - (\sum C_{\text{ff}})^2/n}}}{\sqrt{\frac{\sum \Delta x(x)^2 - (\sum \Delta x(x))^2/n}{\sum C_{\text{ff}}^2 - (\sum C_{\text{ff}})^2/n}}} \quad (4)$$

~~And the uncertainty of R_{gas} is defined as~~

$$U = \frac{\sqrt{\frac{\sum (\Delta x(x) - \Delta x(x)')^2/n}{\sum C_{\text{ff}}^2 - (\sum C_{\text{ff}})^2/n}}}{\sqrt{\frac{\sum (\Delta x(x) - \Delta x(x)')^2/n}{\sum C_{\text{ff}}^2 - (\sum C_{\text{ff}})^2/n}}} \quad (5)$$

~~Here, $\Delta x(x)' = R_{\text{gas}} \times (C_{\text{ff}} - \overline{C_{\text{ff}}}) + \overline{\Delta x(x)}$~~

~~The correlation coefficient is expressed,~~

$$r = \frac{(\sum \Delta x(x) C_{ff} - \frac{\sum \Delta x(x) \sum C_{ff}}{n})^2}{(\sum \Delta x(x)^2 - \frac{(\sum \Delta x(x))^2}{n}) \times (\sum C_{ff}^2 - \frac{(\sum C_{ff})^2}{n})} \quad (6)$$

~~Results for each species are given in Table 1.~~

2.3 HYSPLIT cluster analysis

HYSPLIT trajectories were run using Unified Model-Global Data Assimilation and Prediction System (UM-GDAPS) weather data at 25 km by 25 km horizontal resolution to determine the regions that influence air mass transport to AMY. A total of 70 air-parcel back-trajectories were calculated for 72-h periods at 3-h intervals matching the time of each flask-air sample taken at AMY from May 2014 to August 2016. We assign the sampling altitude as 500 m, since it was demonstrated that HYSPLIT and other particle dispersion back-trajectory models (e.g., FLEXPART) are consistent at 500 m altitude (Li et al., 2014). Cluster analysis of the resulting 70 back-trajectories categorized six pathways through which air parcels arrive at AMY during the time period of interest.

Among the calculated back-trajectories, 67% indicate air masses originating from the Asian continent. Back-trajectories of continental background air (CB) originating in Russia and Mongolia occurred 13% of the time. 23% of the trajectories originated and travelled through

northeast China (CN). The CN region includes Inner Mongolia and Liaoning, one of the most populated regions in China with 43.9 million people in 2012. These CN air masses arrive in South Korea after crossing through western North Korea. 17% of the trajectories are derived from central eastern China around the Shandong area (CE). The CE region contains Shandianzi (SDZ, 40.65° N, 117.12° E, 287 m a.s.l.) located next to the megacities of Beijing and Tianjin, which are some of China's highest CO₂ emitting regions (Gregg et al., 2008). 14% are Ocean Background (OB) derived from the East China Sea. Among them, a few of the trajectories passed over the eastern part of China (such as e.g., over Shanghai) with high altitude (~1000 m). Flow from South Korea also travels through heavily industrialized and/or metropolitan regions in South Korea (Korea Local, KL, 19%) and under stagnant conditions (Polluted Local region, PL, 14%). Some of the KL air-masses have also passed over the East Sea and Japan.

3. Results and discussions

3.1 Observed $\Delta(^{14}\text{CO}_2)$ and portioning of CO₂ into C_{ff} and C_{bio}

AMY $\Delta(^{14}\text{CO}_2)$ values are almost always lower than those observed at NWR, which we consider to be broadly representative of background values for the mid-latitude Northern Hemisphere (Figure 2). NWR $\Delta(^{14}\text{CO}_2)$, which is based on weekly air samples, was in the range 10.0 to 21.2 ‰, with an average $(16.6 \pm 3)\text{‰}$ (1σ , standard deviation) from May 2014 to August 2016. Waliguan (WLG, 36.28° N, 100.9° E, 3816 m a.s.l.), an Asian background GAW station in China, also showed similar $\Delta(^{14}\text{CO}_2)$ levels to NWR with an average of $(17.1 \pm 6.8)\text{‰}$ in 2015

(Niu et al., 2016, measurement uncertainty $\pm 3\text{‰}$, n=20). $\Delta(^{14}\text{CO}_2)$ at AMY varied from -59.5 to 23.1‰ and had a mean value of $(-6.2 \pm 18.8)\text{‰}$ (1σ , n=70) during the ~~experiment~~-measurement period (Table S1). This was similar to results from observations at SDZ, which is located about 100 km northeast of Beijing, in the range of -53.0 to 32.6‰ with an average $(-6.8 \pm 21.1)\text{‰}$ (1σ , n=32) during Sep 2014 to Dec 2015 (Niu et al., 2016).

Calculated C_{ff} at AMY ranges between -0.05 and $32.7 \mu\text{mol mol}^{-1}$ with an average of $(9.7 \pm 7.8) \mu\text{mol mol}^{-1}$ (1σ , n=70); high C_{ff} was observed regardless of season (Figure 2 (a)). One negative C_{ff} value of $-0.05 \mu\text{mol mol}^{-1}$ was estimated due to greater AMY $\Delta(^{14}\text{CO}_2)$ than NWR on July 30, 2014. Although negative C_{ff} values are non-physical, this value is not significantly different from zero, and is reasonable given that this air originated from the OB sector. The range of C_{ff} in the AMY samples is similar to that observed at TAP from 2004 to 2010 (-1.6 to $42.9 \mu\text{mol mol}^{-1}$ C_{ff}), but C_{ff} is on average about twice as high at AMY as in the 2004 to 2010 TAP samples (mean $(4.4 \pm 5.7) \mu\text{mol mol}^{-1}$, n=202) (Turnbull et al., 2011a). A more detailed comparison of results based on differences between samples derived from the Asian continent and Korea local air is provided in section 3.2.

Estimated C_{bio} , as defined in section 2.2.1, varied from -18.1 to $15.7 \mu\text{mol mol}^{-1}$ (mean $(0.9 \pm 5.8) \mu\text{mol mol}^{-1}$) at AMY (Figure 2 (c)). C_{bio} showed a strong seasonal cycle with the lowest values from July to September when photosynthetic drawdown is expected to be strongest, in good agreement with the previous TAP study (Turnbull et al., 2011a). Even though C_{bio} was at times

negative, mainly due to photosynthesis during summer, the largest positive C_{bio} was also observed in summer.

The largest C_{ff} by season was observed in order of winter (DJF, (11.3 ± 7.6) , $n=14$) > summer (JJA, (10.7 ± 9.2) , $n=11$) > spring (MAM, (8.6 ± 8.0) , $n=22$) > autumn (SON, (7.6 ± 5.6) , $n=17$) with a unit of $\mu\text{mol mol}^{-1}$. When we consider only positive contributions of C_{bio} samples, the order was summer $((4.6 \pm 4.0)$, $n=14$) > autumn $((4.1 \pm 2.5)$, $n=9$) > spring $((3.8 \pm 2.6)$, $n=13$) > winter $((3.4 \pm 2.5)$, $n=11$) with a unit of $\mu\text{mol mol}^{-1}$.

C_{ff} in summer was nearly as high as in winter. This is because lower wind speeds are observed at AMY during summer (Lee et al., 2019), ~~), suggesting that these summer high values may reflect emission from local activities, which were described in section 2.1, more than in other seasons.~~ When we analyzed seasonal boundary layer height for each sample by UM-GDAPS, it also showed similar result that it was highest in winter (with a range from 150 m to 1100 m) and lowest in summer (with a range from 100 m to 500 m). This suggests that these high summer C_{ff} values may reflect emission from local activities, which were described in section 2.1, more than in other seasons.

The highest C_{bio} value was also observed in the summer, PL sector. PL sector showed that positive C_{bio} correlates with CH_4 , which is a tracer for agriculture when observed in TAP local air masses. Turnbull et al.(2011a) also showed similar results.

In winter, C_{bio} was relatively lower than in other seasons while C_{ff} was highest. During winter, AMY is mainly affected by long-range transport of air-masses from China due to the Siberian high (Lee et al., 2019). Therefore air samples were less affected by local activities in winter but C_{bio} still contributed almost 23% to $\Delta\chi(\text{CO}_2)$. In the dry season (from October to March), forest

fires, which contribute the largest portion of total CO₂ emissions from open fires at the national scale, are concentrated in northeastern and southern China (Yin et al., 2019). The highest CO₂ was observed in winter ((449.1±244.1) nmol mol⁻¹ (1σ) in winter while (236.8±124.4) nmol mol⁻¹ (1σ) in summer), which also supports biomass burning and bio fuels as large contributors to observed CO₂ enhancements in winter. Turnbull et al. (2011a) also showed that 20-30% of winter CO₂ enhancements at TAP were likely contributed by biofuel combustion, along with plant, soil, human, and animal respiration.

Regardless of the source, we find that C_{bio} contributes substantially to atmospheric CO₂ enhancements at AMY in air masses affected by local and long-range transport, so when only CO₂ enhancements above background are compared to bottom-up inventories, it can make a bias due to C_{bio} contributions.

3.2 C_{ff} comparison between Korea Local and Asian Continent samples

To more clearly identify samples originating from the Asian continent (trajectory clusters CB, CN, CE, and OB) and Korea Local (trajectory cluster KL) after cluster analysis of the 70 sets of measurements, we use wind speed data from the Automatic Weather System (AWS) installed at the same level as the air sample inlet at AMY. Among the data from CB, CN, CE, OB, and KL, when wind speed was less than 3 m/s, we assumed that those samples could be affected by local pollution. PL was also ruled out since it was affected by local pollutions under the stagnant condition. Therefore we use only 41 sets of observations for this analysis (Table 1).

314 C_{ff} is highest in the order CE > CN > KL > CB > OB (Table 1). During the ~~experimental~~
 315 ~~measurement~~ period, the averages from Asian continent (sectors CE and CN) were higher than
 316 KL without the baseline ~~sector (CB and OB)~~. The calculated mean C_{ff} using only CE, CN, CB
 317 and OB, which sample substantial outflow from the Asian Continent, was $(7.6 \pm 3.9) \mu\text{mol mol}^{-1}$.

318 When we compared the KL samples $((8.6 \pm 5.3) \mu\text{mol mol}^{-1})$ with those from Korea Local air-
 319 masses observed at TAP $((8.5 \pm 8.6) \mu\text{mol mol}^{-1})$, ~~n=58~~, Turnbull et al., 2011a), mean C_{ff} was
 320 quite similar (Figure 3). However, when comparing the C_{ff} values from CB air masses in this
 321 study and TAP far-field (from China) samples (~~n=144~~, Turnbull et al., 2011a), C_{ff} almost
 322 doubled from (2.6 ± 2.4) to $(4.3 \pm 2.1) \mu\text{mol mol}^{-1}$, even though they might be expected to have
 323 had similar air mass back-trajectories. We also compared the values at SDZ from 2009 to 2010
 324 (Turnbull et al., 2011a) and in 2015 (Niu et al., 2016); they also increased, not only in the
 325 samples that were affected by Beijing and North China Plain (SDZ-BN), which are comparably
 326 polluted, but also in the samples that were affected by northeast China (SDZ-NE). For SDZ-BN
 327 samples, C_{ff} increased from (10 ± 1) to $(16 \pm 7.6) \mu\text{mol mol}^{-1}$ from 2009/2010 (~~n=32~~) to 2015
 328 (~~n=32~~). The AMY samples from CE, which flow over Beijing, showed $(11.2 \pm 8.3) \mu\text{mol mol}^{-1}$ of
 329 C_{ff} and were also slightly greater than the 2009 – 2010 SDZ-BN samples (Turnbull et al., 2011a).
 330 For SDZ-NE samples, C_{ff} was $(3 \pm 7) \mu\text{mol mol}^{-1}$ in 2009 to 2010 and increased to (7.6 ± 6.8)
 331 $\mu\text{mol mol}^{-1}$ in 2015. Since the SDZ-NE samples are affected by northeast China according to
 332 Turnbull et al. (2011a) and Niu et al. (2016),

we also see CN that originated from northeast china (NE) and its mean value of C_{ff} had increased around $(10.6 \pm 6.9) \mu\text{mol mol}^{-1}$ compared to those values in 2009 to 2010.

It has been suggested that inter-annual variability in observed mean C_{ff} in South Korea could reflect changing fossil fuel CO_2 emissions, or could indicate inter-annual variability in the air mass trajectories of the (small) dataset of flask-air samples (Turnbull et al., 2011a). Even though the growth rate of C_{ff} emission has been decreasing slowly in East Asia since 2010 due to emission reduction policies (Labzovskii et al., 2019), reported emissions increased 16.7% in China and 1.8% in South Korea from 2010 to 2016 (Janssens-Maenhout et al., 2017). This is broadly consistent with the flat trend in observed C_{ff} in ~~Korea-Local~~KL air masses, and in the upward trend in C_{ff} observed in air-masses flowing out from Asia. Therefore it is possible that AMY mean C_{ff} increased relative to the earlier TAP observations due to increased fossil fuel emissions from the Asian continent. ~~It is also likely that the proximity of local emission sources to AMY is causing higher observed C_{ff} under some synoptic conditions.~~

On the other hand, those values from this study showed large variability with small sample numbers due to different sampling strategy, environment, and synoptic conditions such as boundary layer height at the sampling time from reference studies. Further study will be necessary to understand those increased values.

3.3. Correlation of C_{ff} with SF_6 and its emission ratios

We calculated correlation coefficients (r from Equ. (S3)) between SF_6 and CO enhancements with C_{ff} and their ratios from Equ. (S1) with the 50 samples that were described in section 3.2 including PL sector ($n=9$) and whose values are tabulated in Table 1.

The correlations of CO enhancements ($\Delta x(\text{CO})$) with C_{ff} were strong ($r > 0.7$) in all sectors except PL, while SF_6 enhancements ($\Delta x(\text{SF}_6)$) correlated strongly with C_{ff} ($r > 0.8$) for CE and OB in outflow from the Asian Continent and KL. R_{CO} and R_{SF_6} were different between Korea Local and outflows from the Asian Continent. Here we discuss R_{SF_6} and section 3.4 discuss R_{CO} more detail.

For SF_6 , observed mean levels were high in order of (KL, PL) > (CN, CE) > (OB-, CB) (Table 1). SF_6 in KL and PL were higher than from the Asian Continent, since South Korea has larger SF_6 emissions than most countries (ranked at 4th as of 2010 according to the EDGAR4.2.) because of liquid-crystal display (LCD) and electrical equipment production (Fang et al., 2014). Even though ~~South Korea~~ both KL and PL showed higher SF_6 mole fraction than outflows of Asian Continent, the correlation is different between KL and PL (Table 1). Under stagnant conditions, emitted SF_6 is less diluted by mixing, so that in PL, $\Delta x(\text{SF}_6)$ correlated weakly with C_{ff} . On the other hand, KL, CE and OB showed strong correlations ($r > 0.8$). Those three sectors are also larger SF_6 sources compared to other regions, according to SF_6 emission estimates for Asia (Fang et al., 2014). Because long-range transport allows time for mixing, SF_6 and C_{ff} emissions are effectively co-located at not only continental scales but also regional scales. Thus SF_6 can be a good tracer of fossil fuel CO_2 for those regions.

The correlation between $\Delta x(\text{SF}_6)$ and C_{ff} was strong in CE, OB and KL, however, R_{SF_6} is different between South Korea and outflow from the Asian continent (Figure S2). In a previous

study, observed R_{SF_6} was 0.02 to 0.03 $\text{pmol } \mu\text{mol}^{-1}$ at NWR in 2004 (Turnbull et al., 2006). Here, the ratio was at (0.19 ± 0.03) and (0.17 ± 0.03) $\text{pmol } \mu\text{mol}^{-1}$ for CE and OB respectively. For KL, it was (0.66 ± 0.16) $\text{pmol } \mu\text{mol}^{-1}$ indicating much larger ratios than in outflow from the Asian continent. Further, observed R_{SF_6} is 2 to 3 times greater for all air masses than predicted from bottom-up inventories based on national scale roughly. For this calculation, we use EDGAR4.3.2 for CO_2 and EDGAR4.2 for SF_6 . We repeat the calculations for both CO_2 and SF_6 with Korea's National Inventory Report (KNIR, Greenhouse Gas Inventory and Research Center, 2018). Using SF_6 for 2010 from EDGAR4.2, we obtain R_{SF_6} of 0.08 $\text{pmol } \mu\text{mol}^{-1}$ for China while for South Korea it was 0.14 $\text{pmol } \mu\text{mol}^{-1}$. Especially for South Korea, this is much lower than the observed R_{SF_6} . When KL R_{SF_6} was compared to ratios calculated from the KNIR inventory (0.27 $\text{pmol } \mu\text{mol}^{-1}$ for 2010 and 0.22 $\text{pmol } \mu\text{mol}^{-1}$ for 2014), it was closer to observed R_{SF_6} than EDGAR, but still underestimated (Figure S3 and S2). This result suggests that the observed ratio could be used to re-evaluate the bottom-up inventories (Rivier et al., 2006), especially targeting the Asian continent. Even though KL R_{SF_6} showed greater uncertainty than CE and OB, it is still greater than bottom-up inventories, such as KNIR and EDGAR. Therefore it would be useful to get more data to try and derive a more robust estimate to evaluate SF_6 emission inventories in for Korea.

3.4 Correlation of C_{ff} with CO and its emission ratios

High CO was mainly observed in outflow from the Asian continent in order of $\text{CE} > \text{CN} > \text{PL} > (\text{CB}, \text{KL}) > \text{OB}$ (Table 1). The order of CO is quite different to that of SF_6 . CO from KL and PL

is lower than from outflow from the Asian continent, except for the OB sector, indicating that high CO can be a tracer of outflow from the Asian continent. Since CO is produced during incomplete combustion of fossil fuel and biomass, it is more closely related to fossil fuel CO₂ emissions than the other trace gases. Therefore in most cases the correlation between CO and C_{ff} was strong. R_{CO} was very different between air masses originating from South Korea Local ((8±2) nmol μmol⁻¹) and the Asian continent ((29±8) to (36±2) nmol μmol⁻¹), ~~likely~~ due to differences in combustion efficiencies and the use of catalytic converters. The higher continental emission ratios may also result from some contribution of biofuel combustion and agricultural burning in the Asian continent, which have significantly higher CO emission than fossil-fuel combustion (Akagi et al., 2011). For example, for CB the CO level is similar to KL while R_{CO} is higher than KL with low C_{ff}.

Typically CO shows seasonal variations with lower values in summer due to the ~~photochemical sink~~atmospheric chemical sink, OH. Among the samples, the samples collected in summer were mainly rejected through wind speed cut-off (less than 3 m/s) since AMY has lower wind speed in summer (Lee et al., 2019). Only OB sector includes 4 summer samples (of 7), because summer air masses are mainly from the southern part of the Yellow Sea (Lee et al., 2019). However, we assumed R_{CO} is less affected by the summer sink, since only two Δx(CO) samples were negative for OB (Figure S2S1) and R_{CO} was consistent whether or not the negative Δx(CO) values were considered. ~~We compare our R_{CO} to results from previous studies in section 3.4.~~

To compare emission ratios derived from atmospheric observations with those from inventories for 2000 to 2012, we calculated inventory emission ratio (I_{CO/CO2}) as:

$$I_{\text{CO/CO}_2} = E_{\text{CO}}/E_{\text{CO}_2} \times M_{\text{CO}_2}/M_{\text{CO}} \quad (7)$$

Where, E_{CO} and E_{CO_2} are total CO and fossil fuel CO₂ emissions in gigagrams (Gg, 10⁹ g) from the bottom-up national inventory. M_X ~~are~~is the molar masses of CO₆ and CO₂ in g mol⁻¹.

We use EDGAR4.3.2 (Janssens-Maenhout et al., 2017) and KNIR (Greenhouse Gas Inventory and Research Center, 2018) for inventory information for both CO and CO₂.

The uncertainty of EDGAR4.3.2 fossil fuel CO₂ emissions was reported as a 95% confidence interval (Janssens-Maenhout et al., 2019), ±5.4% for China and ±3.6% for South Korea (personal communication with Dr. Efisio Solazzo). The uncertainties of CO and SF₆ emissions were not reported by EDGAR. For KNIR, the CO₂ 2016 emission uncertainty in the energy sector was ±3% (Greenhouse Gas Inventory and Research Center, 2018). KNIR does not provide uncertainties for other emission sectors of CO₂, nor from emissions of CO and SF₆.

In Fig. 4 we confirm that the CO to C_{ff} emission ratios (R_{CO}) derived from both observations and inventories for China and South Korea are decreasing. Since C_{ff} emissions appear to be flat (South Korea) or slightly increasing (China), this indicates that combustion efficiency and/or scrubbing of CO is improving.

For South Korea, EDGAR4.3.2 indicated that CO emissions from the energy sector (98% to 99% of total emission) decreased by 47% between the 1997 and 2012. South Korean fossil fuel CO₂ emissions increased until 2011 and remained mostly constant from 2011 to 2016 ((603,901±4,315) Gg CO₂) (Figure S4). Therefore the decreased trend in the emission ratio

seems to reflect recent decreases in CO emissions in South Korea. Turnbull et al. (2011a) determined an observed mean R_{CO} of (13 ± 3) nmol μmol^{-1} during 2004 to 2010. Suntharalingam et al. (2004) estimated R_{CO} 15.4 nmol μmol^{-1} for South Korea in 2001 from CO_2 and CO airborne observations (C_{ff} was not determined). Recently, the KORUS-AQ campaign, which was conducted over Seoul from May to June in 2016, estimated R_{CO} as 9 nmol μmol^{-1} (Tang et al., 2018) based on CO_2 and CO observations (C_{ff} was not determined). Our study gives R_{CO} of (8 ± 2) nmol μmol^{-1} for South Korea, slightly but not significantly lower than the KORUS-AQ result for Seoul. ~~This difference could be due to different source regions (Seoul vs the larger Korean region) and different experimental periods (two months vs two years).~~ Different contributions of C_{bio} and C_{ff} to total CO_2 may bias the R_{CO} calculation when total CO_2 was used in the KORUS-AQ study (e.g., Miller et al., 2012). The South Korean national R_{CO} from EDGAR4.3.2 in 2012 was 6.7 nmol μmol^{-1} , consistent with our observations. Using KNIR for 2016, we obtain R_{CO} of 2.1 nmol μmol^{-1} . KNIR suffers from a large number of missing CO emission sources compared to the EDGAR, as indicated by their reported emissions, 638.3 and 2580.8 Gg in 2012, respectively (Figure S5). For example, CO emissions recently derived from fugitive emissions and residential/other sectors increased to 14% and 11.5% of total emission respectively in EDGAR but were not reported in KNIR.

For China the inventories estimate that CO emissions from the energy sector, $(96.5 \pm 0.2)\%$, were almost constant through the 1990s, and then increased during the early-2000s from industrial processes (8.8% of total emissions in 2012). Fossil fuel CO_2 emission in China also increased

until 2013 and then stayed roughly constant at $(10,461,890 \pm 60,571)$ Gg according to
 EDGAR4.3.2. Thus even though both emissions show an increase from 2000 to 2016 for fossil
 fuel CO_2 and to 2012 for CO, the emission ratio decreased (Figure S4 and Figure 4) seeming to
 indicate that combustion efficiency is improving. Many studies observed decreasing R_{CO} in
 China from 2000 to 2010 (Turnbull et al., 2011a; Wang et al., 2010). Suntharalingam et al. (2004)
 reported R_{CO} was $55 \text{ nmol } \mu\text{mol}^{-1}$ in 2001 (C_{ff} was not determined). In the Beijing region, R_{CO}
 decreased from 57.80 to $37.59 \text{ nmol } \mu\text{mol}^{-1}$ during 2004 to 2008 (Wang et al., 2010). The overall
 R_{CO} was $(47 \pm 2) \text{ nmol } \mu\text{mol}^{-1}$ at SDZ for 2009-2010 and $(44 \pm 3) \text{ nmol } \mu\text{mol}^{-1}$ in air-masses that
 originated from the Asian continent from 2005 to 2009 (Turnbull et al., 2011a). Tohjima et al.
 (2014) explained that surface based R_{CO} decreased from 45 to $30 \text{ nmol } \mu\text{mol}^{-1}$ in outflow air
 masses from China from 1998 to 2010. Fu et al. (2015) also observed R_{CO} of $29 \text{ nmol } \mu\text{mol}^{-1}$
 over mainland China in 2009. In Beijing, which is located along the path of CE, it was (30.4 ± 1.6)
 $\text{nmol } \mu\text{mol}^{-1}$ and $(29.6 \pm 3.2) \text{ nmol } \mu\text{mol}^{-1}$ for Xiamen in 2016, which is in the OB sector (Niu et
 al., 2018). During KORUS-AQ in 2016, R_{CO} of $28 \text{ nmol } \mu\text{mol}^{-1}$ was observed over the Yellow
 Sea. Some of those studies did not differentiate C_{ff} from the total CO_2 enhancement, so, although
 R_{CO} still includes uncertainties, it is continually decreasing.

In this study R_{CO} is (29 ± 8) , (31 ± 8) , (36 ± 2) , and $(31 \pm 4) \text{ nmol } \mu\text{mol}^{-1}$ for CB, CN, CE and OB,
 consistent with Tang et al.(2018) and Liu et al.(2018). On the other hand, R_{CO} in CE is higher
 than in other sectors in this study. The Shandong area, which is located in the path of CE, has
 been plagued with problems of combustion inefficiency and ranked as the largest consumer of
 fossil fuels in all of China (Chen and Li, 2009). The uncertainties in our observed R_{CO} for this

region overlap with other sectors such as CB, CN and OB, so further monitoring of the ratios will help to get more detailed information.

In South Korea and China, atmosphere-based R_{CO} values calculated by this study are (1.2 ± 0.3) times (with KL), ~~and (1.8 ± 0.2)~~ (1.6 ± 0.4) , (1.7 ± 0.4) , (2 ± 0.1) and (1.7 ± 0.2) times greater (with CB, CN, CE and OB) than in the inventory, respectively (Figure 4). This is in agreement with previous studies (Turnbull et al., 2011a; Kurokawa et al., 2013; Tohjima et al., 2014). One explanation is that EDGAR does not reflect secondary CO production, which can be a significant contributor to CO (Kurokawa et al., 2013). Also, CO derived from biomass burning and biofuels was not included in this inventory. Therefore, this indicates that top-down observations are necessary to evaluate and improve bottom-up emission products.

4. Summary and Conclusions

To understand CO_2 sources and sinks in Korea as well as those of the surrounded region, we collected $\Delta(^{14}CO_2)$ with 70 flask samples from May 2014 to August 2016. We summarized our results below.

- 1) Observed $\Delta(^{14}CO_2)$ values at AMY ranged from -59.5 to 23.1‰ (a mean value of $(-6.2 \pm 18.8)\text{‰}$ (1σ)) during the study period, almost always lower than those observed at NWR, which we consider to be broadly representative of background values for the mid-

latitude Northern Hemisphere. This reflects the strong imprint of fossil fuel-CO₂ emissions recorded in AMY air samples.

1) Calculated C_{ff} using $\Delta(^{14}\text{CO}_2)$ at AMY ranges between -0.05 and 32.7 $\mu\text{mol mol}^{-1}$ with an average of $(9.7 \pm 7.8) \mu\text{mol mol}^{-1}$ (1σ); this average is twice as high as in the 2004 to 2010 TAP samples (mean $(4.4 \pm 5.7) \mu\text{mol mol}^{-1}$) (Turnbull et al., 2011a). We also observed high C_{ff} regardless of the season or source region. After separately identifying samples originating from the Asian continent and the Korean peninsula, we determined that the mean C_{ff} increased relative to the earlier observations due to increased fossil fuel emissions from the Asian continent as showing by the consistent growth in reported emissions, which increased 16.7% in China and only 1.8% in South Korea from 2010 to 2016. Note, however, that our data span a relatively limited time period and are subject to different synoptic conditions during the sampling time from previous studies, so a longer time-series would increase confidence in tracking this change.

2)

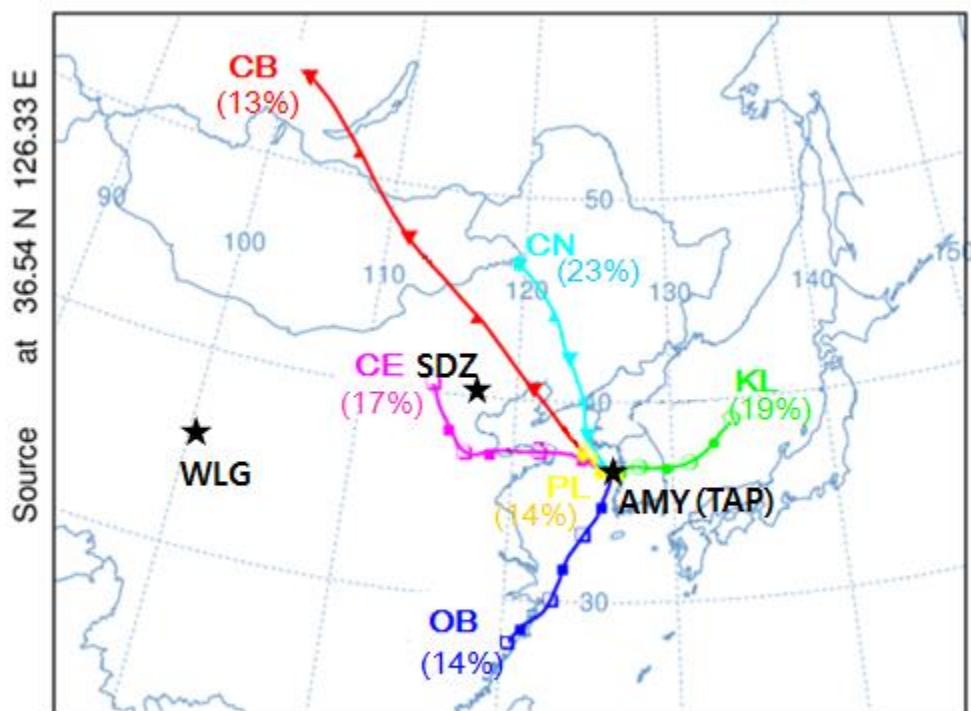
3) Because $\Delta x(\text{CO})$ and $\Delta x(\text{SF}_6)$ agreed well with C_{ff} , but showed different slopes for Korea and the Asian continent, those R_{gas} values can be indicators of air mass origin and those gases can be proxies for C_{ff} . Overall, we have confirmed that both R_{CO} derived from inventory and observation have decreased relative to previous studies, indicating that combustion efficiency is increasing in both China and South Korea.

4) However, a Atmosphere-based R_{gas} values are greater than bottom-up inventories. For CO,
our values are (1.2 ± 0.3) times and (1.6 ± 0.4) to (2 ± 0.1) ~~(1.8 ± 0.2)~~ times greater than in

inventory values for South Korea and China, respectively. This discrepancy may arise from several sources including the absence of atmospheric chemical CO production such as oxidation of CH₄ and non-methane VOCs. Observed R_{SF_6} is 2 to 3 times greater than in inventories. Therefore those values in our study can be used for improving bottom-up inventory-inventories in the future.

2)5) Finally, we stress that because C_{bio} contributes substantially to $\Delta x(\text{CO}_2)$, even in winter, $\Delta^{14}\text{C}$ -based C_{ff} (and not $\Delta x(\text{CO}_2)$) is required for accurate calculation of both R_{CO} and R_{SF_6} .

526



527

528 Figure 1. A total of 70 air-parcel back-trajectories were calculated for 72-h periods at 3-h
 529 intervals from May 2014 to August 2016 using the HYSPLIT model in conjunction with KMA
 530 UM GDAPS data at 25 km by 25 km resolution. Station locations are: WLG (Waliguan, 36.28°
 531 N, 100.9° E, 3816 m a.s.l.), SDZ (Shandianzi, 40.65° N, 117.12° E, 287 m a.s.l.), and AMY
 532 (Anmyeondo, 36.53° N, 126.32° E, 86 m a.s.l.). TAP (Tae-Ahn Peninsula, 36.73° N, 126.13° E,
 533 20 m a.s.l.) is around 28 km northeast from AMY.

534

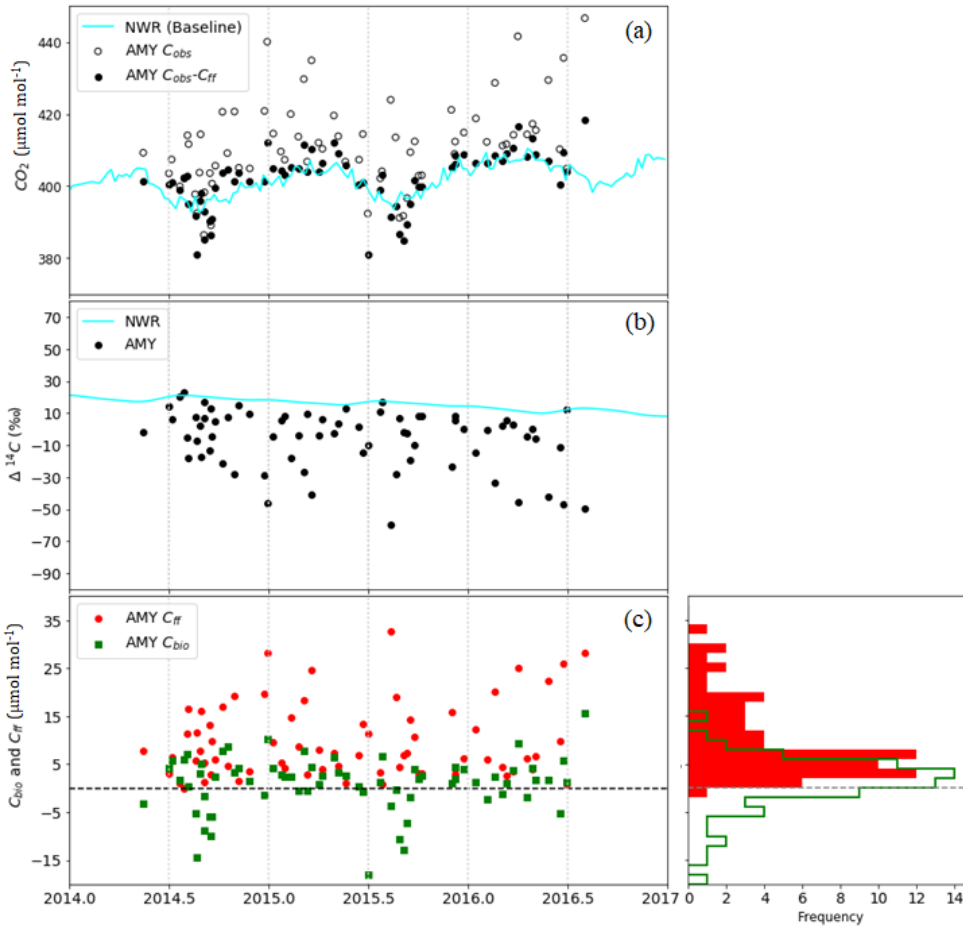
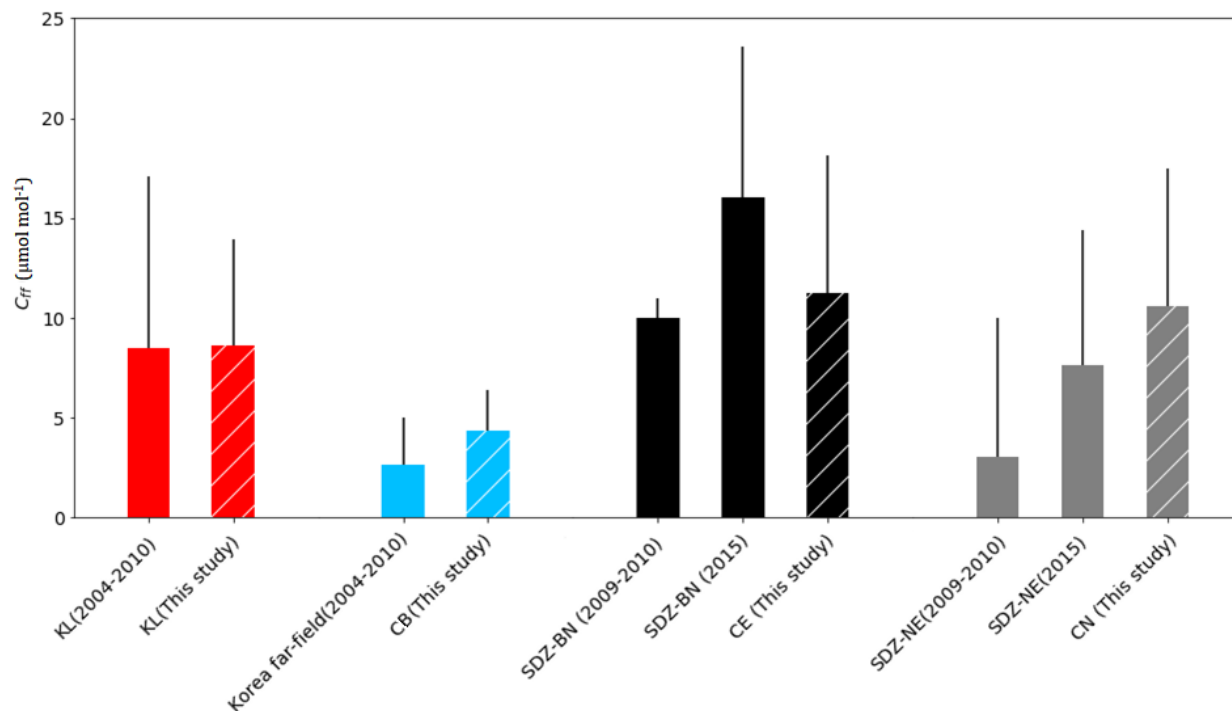


Figure 2. Time series of (a) observed CO_2 dry air mole fraction (open circles) and observed CO_2 (C_{obs}) minus C_{ff} calculated from $\Delta(^{14}\text{CO}_2)$ (closed circles). (b) $\Delta(^{14}\text{CO}_2)$ at AMY (black circles) and at NWR (Niwt Ridge, line), baseline data. (c) Time series of C_{ff} and C_{bio} calculated from $\Delta(^{14}\text{CO}_2)$ (left) and the frequency distribution at AMY (right).



542

543 Figure 3. Calculated C_{ff} ($\mu\text{mol mol}^{-1}$). Red bars are for KL and blue bars are for Korea far-field
 544 (China) (2004-2010 from Turnbull et al. (2011a)). Black bars are for SDZ-BN samples that were
 545 affected by Beijing and North China plain. Gray bars for SDZ-NE indicate samples that were
 546 affected by regions northeast of SDZ. SDZ (2009-2010) is from Turnbull et al. (2011a) and SDZ
 547 (2015) is from Niu et al. (2016). Hatched red, blue, black and grey bars are derived from this
 548 study during 2014 to 2016.

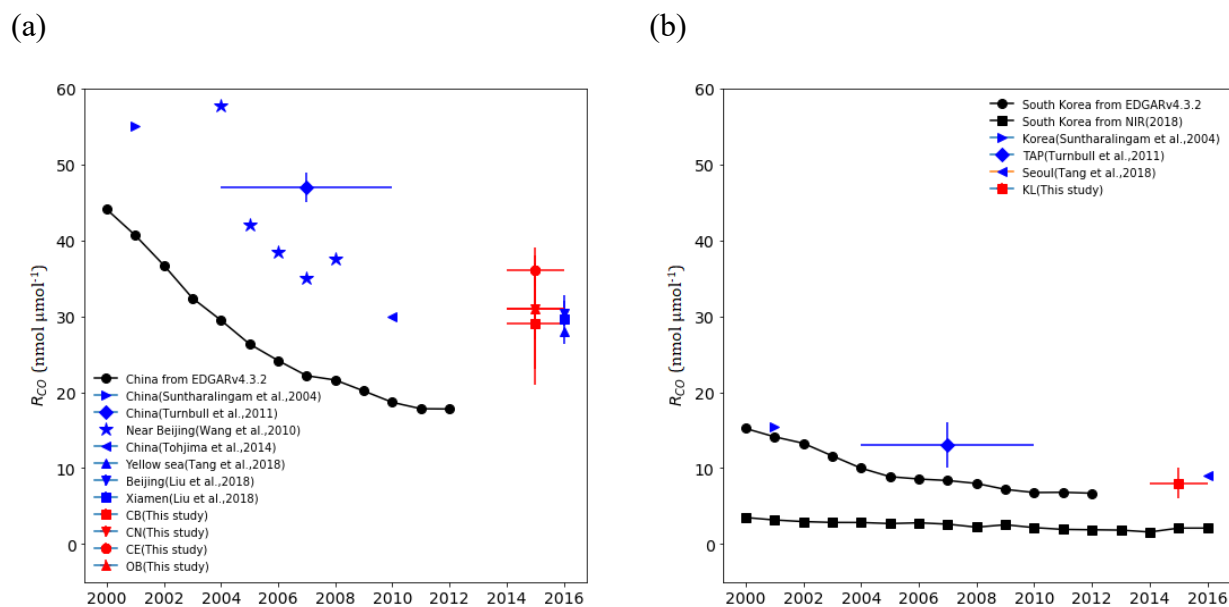


Figure 4. R_{CO} for China (a) and for South Korea (b). Black circles: EDGARv.4.3.2 emission inventory. Black squares: National Inventory Report, Korea (2018). Blue symbols are from other studies (Suntharalingam et al., 2004; Wang et al., 2010; Turnbull et al., 2011a; Tohjima et al., 2014; Liu et al., 2018; Tang et al., 2018). Red symbols: This study. Y-error bars: uncertainty in the slope according to equation (S2). X-error bars: the period for the mean value.

Table 1. Means and standard deviations of C_{ff} ($\mu\text{mol mol}^{-1}$), CO (nmol mol^{-1}) and SF₆ (pmol mol^{-1}) (total N=50, without PL N=41). The correlations (r) and the ratio (R_{gas}) of enhancement between C_{ff} were determined by Reduced Major Axis (RMA) regression analysis on each scatter plot to obtain regression slopes. The uncertainty of R_{gas} refers to equation (S2). When r is less than 0.7, R_{gas} was not included here. N is the number of data. The unit of R_{CO} is $\text{nmol } \mu\text{mol}^{-1}$ and for R_{SF_6} it is $\text{pmol } \mu\text{mol}^{-1}$. A plot of R_{CO} and R_{SF_6} is shown in Figure S1.

	Outflow from the Asia continent				South Korea	
	CB (N=7)	CN (N=9)	CE (N=9)	OB (N=7)	KL (N=9)	PL (N=9)
C_{ff}	4.3 ± 2.1	10.6 ± 6.9	11.2 ± 8.3	4.1 ± 2.7	8.6 ± 5.3	15.6 ± 11.6
CO	233 ± 59	353 ± 219	473 ± 293	169 ± 90	228 ± 40	259 ± 100
SF ₆	9.0 ± 0.4	10.1 ± 1.2	10.1 ± 1.5	9.2 ± 0.5	13.0 ± 3.3	12.7 ± 6.2
R_{CO} (r)	29 ± 8 (0.80)	31 ± 8 (0.76)	36 ± 2 (0.98)	31 ± 4 (0.96)	8 ± 2 (0.74)	- (0.44)
R_{SF_6} (r)	- (0.63)	- (0.48)	0.19 ± 0.03 (0.91)	0.17 ± 0.03 (0.94)	0.66 ± 0.16 (0.76)	- (0.38)

Data availability

Our CO₂, CO, SF₆ data from AMY and NWR can be downloaded from ftp://aftp.cmdl.noaa.gov/data/trace_gases. $\Delta(^{14}\text{CO}_2)$ data are provided in the supplementary material of this paper.

Author contributions

HL wrote this paper and analyzed all data. HL and GWL designed this study. EJD and JCT guided and reviewed this paper. SL collected samples and gave the information of the data at AMY. EJD, JCT, SJL, JBM, GP, and JL provided data and reviewed the manuscript. ~~SSL and YSP reviewed this paper.~~ All authors contributed this work.

ACKNOWLEDGMENT

This work was funded by the Korea Meteorological Administration Research and Development Program "Research and Development for KMA Weather, Climate, and Earth system Services—Development of Monitoring and Analysis Techniques for Atmospheric Composition in Korea" under Grant (1365003041).

REFERENCES

Akagi, S. K., R. J. Yokelson, C. Wiedinmyer, M. J. Alvarado, J. S. Reid, T. Karl, J. D. Crounse, P. O. Wennberg: Emission factors for open and domestic biomass burning for use in atmospheric models, *Atmos. Chem. Phys.* 11, 4039-4027, doi:10.5194/acp-11-4039-2011, **2011**

[Boden, T.A., G. Marland, and R.J. Andres: National CO₂ Emissions from Fossil-Fuel Burning, Cement Manufacture, and Gas Flaring: 1751-2014, Carbon Dioxide Information Analysis Center, Oak Ridge National Laboratory, U.S. Department of Energy, doi 10.3334/CDIAC/00001_V2017, 2017](#)

Chen, Y. Y. Li: Low-carbon economy and China's regional energy use research. *Jilin Univ. J. Soc. Sci. Ed.* 49(2), 66-73, **2009**

Fang, X., R. L. Thompson, T. Saito, Y. Yokouchi, J. Kim, S. Li, K. R. Kim, S. Park, F. Graziosi, A. Stohl: Sulfur hexafluoride (SF₆) emissions in East Asia determined by inverse modeling. *Atmos. Chem. Phys.* 14, 4779–4791, doi:10.5194/acp-14-4779-2014, **2014**

Fu, X. W., H. Zhang, C.-J. Lin, X. B. Feng, L. X. Zhou, S. X. Fang: Correlation slopes of GEM/CO, GEM/CO₂, and GEM/CH₄ and estimated mercury emissions in China, South Asia, the Indochinese Peninsula, and Central Asia derived from observations in northwestern and southwestern China. *Atmos. Chem. Phys.* 15, 1013-1028, doi:10.5194/acp-15-1013-2015, **2015**

Gamnitzer, U., U. Karstens, B. Kromer, R. E. M. Neubert, H. Schroeder, I. Levin: Carbon monoxide: A quantitative tracer for fossil fuel CO₂?. *J. Geophys. Res.*, 111, D22302, doi:10.1029/2005JD006966, **2006**

Geller, L. S., J. W. Elkins, J. M. Lobert, A. D. Clarke, D. F. Hurst, J. H. Butler, R. C. Myers: Tropospheric SF₆: Observed latitudinal distribution and trends, derived emissions and interhemispheric exchange time. *Geophys. Res. Lett.*, 24(6), 675–678, doi:10.1029/97GL00523, **1997**

605 Graven, H. D. N. Gruber: Continental-scale enrichment of atmospheric $^{14}\text{CO}_2$ from the nuclear
606 power industry: Potential impact on the estimation of fossil fuel-derived CO_2 . *Atmos. Chem.*
607 *Phys. Discuss. 11*, 14,583–14,605, doi:10.5194/acpd-11-14583-2011, **2011**

608 Graven, H. D., B. B. Stephens, T. P. Guilderson, T. L. Campos, D. S. Schimel, J. E. Campbell, R.
609 F. Keeling: Vertical profiles of biospheric and fossil fuel-derived CO_2 and fossil fuel $\text{CO}_2:\text{CO}$
610 ratios from airborne measurements of ^{14}C , CO_2 and CO above Colorado, USA, *Tellus*, *61*, 536–
611 546, DOI:10.1111/j.1600-0889.2009.00421.x, **2009**

612 Gregg, J. S. R. J. Andres, G. Marland: China: Emissions pattern of the world leader in CO_2
613 emissions from fossil fuel consumption and cement production, *Geophys. Res. Lett.* *35*, L08806,
614 doi:10.1029/2007GL032887, **2008**

615 Greenhouse Gas Inventory and Research Center: National Greenhouse Gas Inventory Report of
616 Korea; National statistics-115018, 11-1480906-000002-10,
617 www.gir.go.kr/home/index.do?menuId=36 (in Korean), **2018**

618 Hsueh, D. Y., N. Y. Krakauer, J. T. Randerson, X. Xu, S. E. Trumbore, J. R. Southon: Regional
619 patterns of radiocarbon and fossil fuel derived CO_2 in surface air across North America, *Geophys.*
620 *Res. Lett.*, *34*, L02816, doi:10.1029/2006GL027032, **2007**

621 Janssens-Maenhout, G., M. Crippa, D. Guizzardi, M. Muntean, E. Schaaf, J.G.J. Olivier,
622 J.A.H.W. Peters, K.M. Schure: Fossil CO_2 and GHG emissions of all world countries, EUR
623 28766 EN, Publications Office of the European Union, Luxembourg, ISBN 978-92-79-73207-2,
624 doi:10.2760/709792, JRC107877, **2017**

625 Janssens-Maenhout, G.; M. Crippa, D. Guizzardi, M. Muntean, E. Schaaf, F. Dentener, P.
 626 Bergamaschi, V. Pagliari, J. G. J. Olivier, J. A. H. W. Peters, J. A. van Aardenne, S. Monni, U.
 627 Doering, A. M. R. Petrescu, E. Solazzo, G. D. Oreggioni: EDGAR v4.3.2 Global Atlas of the
 628 three major greenhouse gas emissions for the period 1970–2012, *Earth Syst. Sci. Data*, *11*, 959–
 629 1002, <https://doi.org/10.5194/essd-11-959-2019>, **2019**

630 Kurokawa, J., T. Ohara, T. Morikawa, S. Hanayama, G. Janssens-Maenhout, T. Fukui, K.
 631 Kawashima, H. Akimoto: Emissions of air pollutants and greenhouse gases over Asian
 632 regions during 2000–2008: Regional Emission inventory in ASia (REAS) version 2, *Atmos.*
 633 *Chem. Phys.* *13*, 11019–11058, doi:10.5194/acp-13-11019-2013, **2013**

634 Labzovskii, L.D., H. W. L. Mak, S. T. Keneaa, J.-S. Rhee, A. Lashkari, S. Li, T.-Y. Goo, Y.-S.
 635 Oh, Y.-H. Byun: What can we learn about effectiveness of carbon reduction policies from
 636 interannual variability of fossil fuel CO₂ emissions in East Asia? *Environ. Sci. Policy*. *96*, 132–
 637 140, <https://doi.org/10.1016/j.envsci.2019.03.011>, **2019**

638 Lee, H., S.-O. Han, S.-B. Ryoo, J.-S. Lee, G.-W. Lee: The measurement of atmospheric CO₂ at
 639 KMA GAW regional stations, its characteristics, and comparisons with other East Asian sites.
 640 *Atmos. Chem. Phys.* *19*, 2149–2163, doi.org/10.5194/acp-19-2149-2019, **2019**

641 Lehman, S.J., J. B. Miller, C. Wolak, J.R. Southon, P.P. Tans, S.A. Montzka, C. Sweeney, A. E.
 642 Andrews, B.W. LaFranchi, T. P. Guilderson: Allocation of terrestrial carbon sources using ¹⁴CO₂:
 643 methods, measurement, and modelling. *Radiocarbon*. *55*(2–3):1484–95, **2013**

644 Le Quéré, C., R. M. Andrew, P. Friedlingstein, S. Sitch, J. Hauck, J. Pongratz, P. A. Pickers, J. I.
 645 Korsbakken, G. P. Peters, J. G. Canadell, A. Arneeth, V. K. Arora, L. Barbero, A. Bastos, L. Bopp,

646 F. Chevallier, L. P. Chini, P. Ciais, S. C. Doney, T. Gkritzalis, D. S. Goll, I. Harris, V. Haverd, F.
647 M. Hoffman, M. Hoppema, R. A. Houghton, G. Hurtt, T. Ilyina, A. K. Jain, T. Johannessen, C. D.
648 Jones, E. Kato, R. F. Keeling, K. K. Goldewijk, P. Landschützer, N. Lefèvre, S. Lienert, Z. Liu,
649 D. Lombardozzi, N. Metzl, D. R. Munro, J. E. M. S. Nabel, S. Nakaoka, C. Neill, A. Olsen, T.
650 Ono, P. Patra, A. Peregon, W. Peters, P. Peylin, B. Pfeil, D. Pierrot, B. Poulter, G. Rehder, L.
651 Robertson, E.M. Rocher, C. Rödenbeck, U. Schuster, J. Schwinger, R. Séférian, I. Skjelvan, T.
652 Steinhoff, A. Sutton, P. P. Tans, H. Tian, B. Tilbrook, F. N. Tubiello, I. T. vander Laan-Luijkx,
653 G. R. vander Werf, N. Viovy, A. P. Walker, A.J. Wiltshire, R. Wright, S. Zaehle, Bo. Zheng:
654 Global Carbon Budget 2018. *Earth Syst. Sci. Data*. 10, 2141–2194, [https://doi.org/10.5194/essd-](https://doi.org/10.5194/essd-10-2141-2018)
655 [10-2141-2018](https://doi.org/10.5194/essd-10-2141-2018), **2018**

656 Levin, I., B., M. S. Kromer, H. Sartorius: A novel approach for independent budgeting of fossil
657 fuel CO₂ over Europe by ¹⁴CO₂ observations, *Geophys. Res. Lett.* 30(23), 2194,
658 doi:10.1029/2003GL018477, **2003**

659 Li, S., J. Kim, S. Park, S.-K. Kim, M.-K. Park, J. Mühle, G.-W. Lee, M. Lee, C. O. Jo, K.-R.
660 Kim: Source identification and apportionment of halogenated compounds observed at a remote
661 site in East Asia. *Environ. Sci. Technol.* 48, 491–498, doi.org/10.1021/es402776w, **2014**

662 Miller, J.B., S. J. Lehman, S. A. Montzka, C. Sweeney, B. R. Miller, A. Karion, C. Wolak, E. J.
663 Dlugokencky, J. Southon, J. C. Turnbull, P.P. Tans: Linking emissions of fossil fuel CO₂ and
664 other anthropogenic trace gases using atmospheric ¹⁴CO₂. *J. Geophys. Res.* 117, D08302,
665 doi:10.1029/2011JD017048, **2012**

666 Niu, Z., W. Zhou, X. Feng, T. Feng, S. Wu, P. Cheng, X. Lu, H. Du, X. Xiong, Y. Fu:
667 Atmospheric fossil fuel CO₂ traced by ¹⁴CO₂ and air quality index pollutant observations in

668 Beijing and Xiamen, China. *Environ. Sci. Pollut. Res.* 25, 17109–17117,
669 doi.org/10.1007/s11356-018-1616-z, **2018**

670 Niu, Z., W. Zhou, P. Cheng, S. Wu, X. Lu, X. Xiong, H. Du, Y. Fu: Observations of atmospheric
671 $\Delta^{14}\text{CO}_2$ at the global and regional background sites in China: Implication for fossil fuel CO_2
672 inputs. *Eviron. Sci. Technol.* 50, 12122–12128 DOI: 10.1021/acs.est.6b02814, **2016**

673 Nydal, R., and K. Lövseth, Carbon-14 measurements in atmospheric CO_2 from Northern and
674 Southern Hemisphere sites, 1962–1993, technical report, *Carbon Dioxide Inf. Anal. Cent., Oak*
675 *Ridge Natl. Lab.*, U.S. Dep. of Energy, Oak Ridge, Tenn, **1996**

676 Rafter, T. A., and G. J. Fergusson, “Atom Bomb Effect”—Recent increase of Carbon-14 content
677 of the atmosphere and biosphere, *Science*, 126(3273), 557–558, **1957**

678 Palstra, S. W., U. Karstens, H.-J. Streurman, H. A. J. Meijer: Wine ethanol ^{14}C as a tracer for
679 fossil fuel CO_2 emissions in Europe: Measurements and model comparison, *J. Geophys. Res.*,
680 113, D21305, doi:10.1029/2008JD010282, **2008**

681 Riley, W. G., D. Y. Hsueh, J. T. Randerson, M. L. Fischer, J. Hatch, D. E. Pataki, W. Wang, M.
682 L. Goulden: Where do fossil fuel carbon dioxide emissions from California go? An analysis
683 based on radiocarbon observations and an atmospheric transport model, *J. Geophys. Res.*, 113,
684 G04002, doi:10.1029/2007JG000625, **2008**

685 Rivier, L., P. Ciais, D. A. Hauglustaine, P. Bakwin, P. Bousquet, P. Peylin, A. Klonecki:
686 Evaluation of SF_6 , C_2Cl_4 , and CO to approximate fossil fuel CO_2 in the Northern Hemisphere
687 using a chemistry transport model. *J. Geophys. Res.* 111, D16311, doi:10.1029/2005JD006725,
688 **2006**

689 Suntharalingam, P., D. J. Jacob, P. I. Palmer, J. A. Logan, R.M. Yantosca, Y. Xiao, M. J. Evans:
 690 Improved quantification of Chinese carbon fluxes using CO₂/CO correlations in Asian outflow, *J.*
 691 *Geophys. Res.* 109, D18S18, doi:10.1029/2003JD004362, **2004**

692 Suess, H. E. Radiocarbon concentration in modern wood, *Science*, 122,415, **1955**

693 Stuiver, M., P. Quay: Atmospheric ¹⁴C changes resulting from fossil fuel CO₂ release and cosmic
 694 ray flux variability, *Earth Planet. Sci. Lett.* 53, 349–362, **1981**

695 Tang, W., A. F. Arellano, J. P. DiGangi, Y. Choi, G. S. Diskin, A. Agustí-Panareda, M.
 696 Parrington, S. Massart, B. Gaubert, Y. Lee, D. Kim, J. Jung, J. Hong, J.-W. Hong, Y. Kanaya, M.
 697 Lee, R. M. Stauffer, A. M. Thompson, J. H. Flynn, J.-H. Woo: Evaluating high-resolution
 698 forecasts of atmospheric CO and CO₂ from a global prediction system during KORUS-AQ field
 699 campaign. *Atmos. Chem. Phys.* 18, 11007–11030, doi.org/10.5194/acp-18-11007-2018, **2018**

700 Tans, P. P.; J. A. Berry, R. F. Keeling: Oceanic ¹³C/¹²C observations: A new window on ocean
 701 CO₂ uptake. *Global Biogeochem. Cycles.* 7(2), 353–368, doi:10.1029/93GB00053, **1993**

702 [Sokal, R. R., and F. J. Rohlf. 1981. Biometry. 2nd edition. Freeman, NY.](#)

703 [Song Jinming, Baoxiao Qu, Xuegang Li, Huamao Yuan, Ning Li, Liqin Duan: Carbon](#)
 704 [sinks/sources in the Yellow and East China Seas-Air-sea interface exchange, dissolution in](#)
 705 [seawater, and burial in sediments. *Science China Earth Sciences.* 61, 1583-1593, **2018**](#)

706 Stuiver, M., Polach H. A. Discussion: Reporting of ¹⁴C data, *Radiocarbon*, 19(3), 355–363, **1977**

707 Tans, P.P., A.F.M. de Jong, W.G. Mook: Natural atmospheric ¹⁴C variation and the Suess effect,
 708 *Science*, 280, 826-828, **1979**

709 Thoning, K. W., P. P. Tans, W. D. Komhyr: Atmospheric Carbon dioxide at Mauna Loa
 710 Observatory 2. Analysis of the NOAA GMCC Data, 1984–1985, *J. Geophys. Res.* *94*, 8549–
 711 8565, **1989**

712 Tohjima, Y., M. Kubo, C. Minejima, H. Mukai, H. Tanimoto, A. Ganshin, S. Maksyutov, K.
 713 Katsumata, T. Machida, K. Kita: Temporal changes in the emissions of CH₄ and CO from China
 714 estimated from CH₄/CO₂ and CO/CO₂ correlations observed at Hateruma Island. *Atmos. Chem.*
 715 *Phys.* *14*, 1663–1677, doi:10.5194/acp-14-1663-2014, **2014**

716 Turnbull, J., P. Rayner, J. Miller, T. Naegler, P. Ciais, A. Cozic: On the use of ¹⁴CO₂ as a tracer
 717 for fossil fuel CO₂: Quantifying uncertainties using an atmospheric transport model, *J. Geophys.*
 718 *Res.* *114*, D22302, doi:10.1029/2009JD012308, **2009**

719 Turnbull, J. C., S. J. Lehman, J. B. Miller, R. J. Sparks, J. R. Southon, P. P. Tans: A new high
 720 precision ¹⁴CO₂ time series for North American continental air. *J. Geophys. Res.* *112*, D11310,
 721 doi:10.1029/2006JD008184, **2007**

722 Turnbull, J. C., P. P. Tans, S. J. Lehman, D. Baker, T. J. Conway, Y. S. Chung, J. Gregg, J. B.
 723 Miller, J. R. Southon, L.-X. Zhou: Atmospheric observations of carbon monoxide and fossil fuel
 724 CO₂ emissions from East Asia. *J. Geophys. Res.*, *116*, D24306, doi:10.1029/2011JD016691,
 725 **2011a**

726 Turnbull, J. C., A. Karion, M. L. Fischer, I. Faloona, T. Guilderson, S. J. Lehman, B. R. Miller, J.
 727 B. Miller, S. Montzka, T. Sherwood, S. Saripalli, C. Sweeney, P. P. Tans: Assessment of fossil
 728 fuel carbon dioxide and other anthropogenic trace gas emissions from airborne measurements

729 over Sacramento, California in spring 2009, *Atmos. Chem. Phys.* 11(2), 705–721,
730 doi:10.5194/acp-11-705-2011, **2011b**

731 Turnbull, J. C. J. B. Miller, S. J. Lehman, P. P. Tans, R. J. Sparks, J. Southon: Comparison of
732 $^{14}\text{CO}_2$, CO, and SF_6 as tracers for recently added fossil fuel CO_2 in the atmosphere and
733 implications for biological CO_2 exchange, *Geophys. Res. Lett.*, 33, L01817,
734 doi:10.1029/2005GL024213, **2006**

735 [Van Der Laan, S, U. Karstens, R.E.M . Neubert, I.T. Van Der Laan-Luijkx and H.A.J. Meijer:](#)
736 [Observation-based estimates of fossil fuel-derived \$\text{CO}_2\$ emissions in the Netherlands using \$\Delta^{14}\text{C}\$,](#)
737 [CO and \$^{222}\text{Rn}\$, *Tellus B: Chemical and Physical Meteorology*, 62:5, 389-402,](#)
738 [DOI:10.1111/j.1600-0889.2010.00493.x. 2010](#)

739 Wang, Y. J. W. Munger, S. Xu, M. B. McElroy, J. Hao, C. Nielsen, H. Ma: CO_2 and its
740 correlation with CO at a rural site near Beijing: Implications for combustion efficiency in China,
741 *Atmos. Chem. Phys.* 10, 8881–8897, doi:10.5194/acp-10-8881-2010, **2010**

742 Yin, L., P. Du, M. Zhang, M. Liu, T. Xu, Y. Song: Estimation of emissions from biomass
743 burning in China (2003–2017) based on MODIS fire radiative energy data, *Biogeosciences*, 16,
744 1629–1640. **2019**

745 [Zondervan, A., and Meijer, H. A. J: Isotopic characterization of \$\text{CO}_2\$ sources during regional](#)
746 [pollution events using isotopic and radiocarbon analysis, *Tellus B: Chemical and Physical*](#)
747 [*Meteorology*, 48\(4\), 601–612, doi:10.1034/j.1600-0889.1996.00013.x, 1996](#)